Ministry of National Infrastructures
Energy and Water Resources
Geological Survey of Israel

Defining and mapping capable tectonic sources for seismic hazard estimation in Israel: general analysis and specific focus for nuclear power plants in Israel

1st Year Report – November 2015

Ittai Kurzon and Nadav Wetzler

Report No. **GSI/21/2015** Jerusalem, November 2015 **RD-27-15**

Ministry of National Infrastructures
Energy and Water Resources
Geological Survey of Israel

Defining and mapping capable tectonic sources for seismic hazard estimation in Israel: general analysis and specific focus for nuclear power plants in Israel

1st Year Report – November 2015

Improving the locations of 30 years of seismic record and obtaining a better estimation of the seismogenic zones along the Dead Sea Fault

Ittai Kurzon and Nadav Wetzler

Ministry of National Infrastructures, Energy and Water Resources Grants:
#212-17-003 and #214-11-010

Report No. **GSI/21/2015** Jerusalem, November 2015 **RD-27-15**

1. Publication No. **RD-27-15**	2.	3. Recipient Accession No.
4.Title: **Defining and mapping capable tectonic sources for seismic hazard estimation in Israel: general analysis and specific focus for nuclear power plants in Israel.** 1st Year Report: **Improving the locations of 30 years of seismic record and obtaining a better estimation of the seismogenic zones along the Dead Sea Fault**	5.Publication Date November, 2015 6. Performing Organiz. Code	
7. Author (s) **Ittai Kurzon, Nadav Wetzler**	8. Performing Organiz. Rep. No. **GSI/21/2015**	
9. Performing Organization Name and Address **Geological Survey of Israel, Jerusalem 95501**	10. Project/ Task / Work Unit No. 11. Contract No**. 214-11-010**	
12.Sponsoring Organization (s) Name and Address The Ministry Of National Infrastructures P.O.B. 13106, 91360 Jerusalem	13. Type of report and period covered 1st Year Report 14. Sponsoring Organiz. Code	
15. Supplementary Note:		

16. **Abstract:** More than 15,000 seismic events were recorded by the Israel Seismic Network (ISN) during the past 30 years, at the vicinity of the Dead Sea Fault (DSF) zone. During those years locations were obtained using several velocity models, which resulted in inconsistence locations. In addition, we found that seismicity is biased to very shallow depth estimations that do not match other estimations of more localized studies in the region. Thus, improving the location of the seismic record is a necessary and sufficient condition, required for the determination of the properties of the capable tectonic sources in the region of Israel, and to estimate their potential hazard. This study is focused on improving the regional earthquake catalog using robust single event location software (within the Antelope software), based on local (after Gitterman et. al., 2005) and global seismic velocity models. The new relocations show more reasonable depth distributions, in accordance with the seismo-tectonic settings of the region. We also demonstrate and analyze the difference in the event-station distribution, showing location effects of a sparse network, in which the main effect is seen for the focal depths: events located out-of-the-network coverage tend to obtain a focal depth shallower than events located within the network coverage; hence, the out-of-the-network events, are less constrained, resulting in higher location uncertainties. The depth cross-section along the DSF zone within the boundaries of this study presents a good correlation with previous estimation of the boundaries of the seismogenic zone, obtained by heat-flow analysis. The relocated earthquake catalogue is regarded as the new initial robust locations of the seismic bulletin of the ISN, and considered as the basis for future studies and for more elaborated relocations; it will be soon open to the public and available for download from the Geological Survey of Israel (GSI) website at: **<https://www.gsi.gov.il>**. This first stage of our project was summarized and accepted to publication in the Seismological Research Letters (SRL), and is attached as an Appendix to this report.

17. **Keywords:** Dead Sea Fault; Relocations of seismic events; Seismogenic zone; Seismogenic depth; Velocity model; Israel earthquake catalogue
העתק ים המלח ; איכון אירועים סיסמיים ; אזורים סיסמוגנים ; עומק סיסמוגני ; מודל מהירויות ; קטלוג רעידות אדמה בישראל

18. Availability Statement	19. Security Class	20. Security Class
	21. 69 Pages	22. Price

Abstract

More than 15,000 seismic events were recorded by the Israel Seismic Network (ISN) during the past 30 years, at the vicinity of the Dead Sea Fault (DSF) zone. During those years locations were obtained using several velocity models, which resulted in inconsistence locations. In addition, we found that seismicity is biased to very shallow depth estimations that do not match other estimations of more localized studies in the region. Thus, improving the location of the seismic record is a necessary and sufficient condition, required for the determination of the properties of the capable tectonic sources in the region of Israel, and to estimate their potential hazard. This study is focused on improving the regional earthquake catalog using robust single event location software (within the Antelope software), based on local (after Gitterman et. al., 2005) and global seismic velocity models. The new relocations show more reasonable depth distributions, in accordance with the seismo-tectonic settings of the region. We also demonstrate and analyze the difference in the event-station distribution, showing location effects of a sparse network, in which the main effect is seen for the focal depths: events located out-of-the-network coverage tend to obtain a focal depth shallower than events located within the network coverage; hence, the out-of-the-network events, are less constrained, resulting in higher location uncertainties. The depth cross-section along the DSF zone within the boundaries of this study presents a good correlation with previous estimation of the boundaries of the seismogenic zone, obtained by heat-flow analysis.

The relocated earthquake catalogue is regarded as the new initial robust locations of the seismic bulletin of the ISN, and considered as the basis for future studies and for more elaborated relocations; it will be soon open to the public and available for download from the Geological Survey of Israel (GSI) website at: <https://www.gsi.gov.il>. This first stage of our project was summarized and accepted to publication in the Seismological Research Letters (SRL), and is attached as an Appendix to this report.

Introduction

Large-scale observations of spatial patterns of earthquake hypocenters show that seismicity is located mainly along plate boundaries (Lay and Wallace, 1995). For smaller scales, such as for regional or local seismic activity, this seismo-tectonic relation is more obscured, and requires higher resolutions of the sub-plate boundaries and fault systems, and an accurate earthquake locations, in order to clearly observe it (e.g., Shearer and Hauksson 2005, Hauksson et al. 2012). Therefore, as we try to extract more information from seismicity patterns, we soon face the issue of how precise is the earthquake catalogue we are examining.

One of the main issues in characterizing fault systems is to determine the seismogenic zones, in which strains are accommodated mainly by brittle failure. The seismogenic zone is affected by many variables; from regional and local stress fields (e.g., Plenefisch and Bonjer, 1997; de Vicente et al., 2008; Palano et al., 2013), through lateral and vertical lithological changes (Aldersons et al., 2003; Brothers et al., 2009), to heat flux ascending from the mantle (Lachenbruch et al., 1985; Grall et al., 2012; Shalev et al., 2013). The base of the seismogenic zone is theoretically determined from the brittle-ductile transition and commonly set between 300 and 350 °C (e.g., Shalev et al., 2013). Therefore in order to properly determine the observed seismogenic zone (e.g., Sibson, 1982) it is crucial that the seismic depths within an earthquake catalogue are well constrained. Due to the mathematical nature of the location problem, depth has lower accuracy than the epicenter, and is highly sensitive to the applied velocity model. Therefore, besides the general issue of improving earthquake locations (e.g., Allam et al., 2014), the issue of improving their focal depths is very significant for the characterization of active seismogenic zones. Similar to the general expectation that the epicenters will fall in close proximity to surface fault traces, we would expect that the hypocenters will have depth distribution reflecting the lithology, fault structure, and other measures observed in the examined region (e.g., heat flux).

The Israeli Seismic Network (ISN) has been established in 1983 (Shapira and Hofstetter, 2007), and was expanded and upgraded several times, following the technological developments in Seismometry. The network monitors the region, providing specifically good coverage of the Dead Sea Fault (DSF) system and the

Carmel Fault System (CFS). During the past 30 years several velocity models were applied to locate the seismic activity (later inserted into JStar, the local software), and several location algorithms were applied; all leading to inconsistent seismic locations. The current data-processing procedure includes an initial automatic detection and location of seismic events, shortly followed by a) analyst review and fine tuning of the P and S detection, b) relocation and c) magnitude estimation. In the process of a current upgrade of the system we reviewed the seismic catalogue recorded through the years, and found that there is a bias to very shallow depth estimations, that do not match other observations that are known from more localized studies in the region (Hofstetter et al., 1996; Aldersons et al., 2003; Hofstetter et al., 2012; Wetzler et al., 2014), and to the observations seen in other similar seismo-tectonic regions (e.g., Sato et al., 2004; Shearer et al., 2005; Zaliapin and Ben-Zion, 2013).

Our first order solution was to revisit the locations of the entire seismic catalogue, assuming that the P and S picks are valid, using a single robust velocity model of the region, and applying a high quality location algorithm, with world-wide distribution. To achieve this goal we applied the ***relocate*** algorithm and the ***GENLOC*** library, of the Antelope package (<https://www.brtt.com>). The results and initial analysis provided in the following text, establish a renewed earthquake catalogue, with better locations, and more reasonable depth distribution.

Geological Background

The crustal structure of Israel is characterized by southeast declining Moho boundary, sub-parallel to the Israeli coastline, associated with a transition zone between the relatively thin intermediate crust of the Eastern Mediterranean Sea (20 km depth) and the thicker crust of Jordan (32 km depth) (Segev et al., 2006). This structure was retrieved by the compilation of several studies including: inversion of teleseismic P waves (Hofstetter et al., 2000), refraction profiles (Ginzburg et al., 1979; Makris et al., 1983; Ben-Avraham et al., 2002; Weber et al., 2004; Koulakov and Sobolev, 2006) and gravity and magnetic maps (Rybakov et al., 1997; Segev et al., 2006).

Israel is also located closely to a large fault system, the Dead Sea Transform (DST), extending from the southern Red Sea spreading center to the northern zone of

plate convergence in southern Turkey, a distance of ~1,000 km, defining the plate boundary between the Arabian and African-Sinai plates (Figure 1). The left-lateral slip motion along the DST has accommodated horizontal displacement of ~100 km (Quennell, 1956; Garfunkel et al., 1981; Garfunkel, 2014), in a mean slip motion of ~5 mm/year (Sadeh et al., 2012) since the Early Miocene. The tectonic activity along the DST has formed a series of deep basins: the Gulf of Eilat (Aqaba), the Sea of Galilee and the Dead Sea Basin, which is the largest and deepest of these basins. The Carmel-Gilboa-Faria fault system is an additional fault system, located at northern Israel (Figure 1), and striking NW-SE, diagonally to the DST, and was suggested to precede the DST, developing during the Senonian (Segev and Rybakov, 2011).

The recent 30 years of on going tectonic activity along the major regional fault system is demonstrated by the seismicity presented in Figure 2. The seismicity pattern highlights the plate boundaries showing localized seismicity along the DST, and the branching of the transform fault system northwards to Lebanon with the Rohm, Yammuneh, and Serghya Faults (Ron, 1987; Lyakhovsky et al., 1994).

The strongest recorded event in the last 160 years was the 1995, Mw 7.2 earthquake, that was followed by 6 months of intense aftershock activity, and was interpreted as a strike-slip fault (Baer et al., 2008). Paleoseismological studies demonstrate that moderate to large magnitude (M > 7) earthquakes occurred along the DST (Shapira et al., 1993; Marco et al., 1996; Marco and Agnon, 2005; Agnon et al., 2006; Wetzler et al., 2010; Lazar et al., 2010). In addition, historical records attest to the occurrence of moderate to strong earthquakes along the DST, which caused extensive damage to historical settlements, observed at damaged structures throughout the region (Marco, 2008).

Previous seismological studies have demonstrated a relatively deep seismogenic activity, located in the Dead Sea area, indicating focal depths down to ~25 km (Aldersons et al., 2003; Hofstetter et al., 2012; Wetzler et al., 2014). These observations, as well as surface heat flux measurements indicate a cold crust, characterized by deep brittle failure (Shalev et al., 2013).

Dataset and Data Processing

Seismological dataset

We reprocessed the seismic activity of the Dead Sea Fault region, from 1985 to 2015, within a geographic rectangle of 33-37 in longitudes, and 28-34 in latitudes. This dataset includes 15,856 earthquakes (Figure 1), in the magnitude range of $0.5 \leq M_d \leq 7.2$, collected by the Geophysical Institute of Israel (GII). The GII has been monitoring the seismic activity in the region during the past 30 years, using the ISN (Figure 1b) consisting of a total of ~ 140 seismic stations; during these years many of these stations were modified: some were de-activated, others upgraded to 3-channel component digital seismometers, and some are still operating similar to their original settings. Since the ISN includes various types of seismometers, the sampling rates in the seismic station vary between 20 sps for the older stations to 100 sps for the modern ones. The current data acquisition system, operated and maintained by the Division of Seismology of the GII, incorporates the ISN stations, two CTBT stations (Comprehensive Nuclear Test-Ban Treaty), and several CNF stations (Cooperating National Facility). A significantly smaller percentage of the data is incorporated from other regional networks: a) GE, Geophone global network of GFZ, b) JSO, the Jordanian Seismic Observatory, and c) CQ, the seismic network of Cyprus.

Data processing

The earthquake bulletin includes the origin location of the seismic events, their origin time, and the P- and S- wave arrival times reviewed and refined by GII's analysts. In addition, it holds the error estimations of the locations, based on the picking errors of the arrival times, assigned by the analysts, and errors due the location algorithm and the velocity model (Polozov and Pinsky, 2004). We regarded the arrival times as the most reliable measure we have, and examined the remaining components, mainly focusing on the velocity model used for the relocations.

Relocation method

We applied the ***relocate*** program of the Antelope software. The program is an end-user interface to the Generalized Location (GENLOC) Library of Antelope software (<www.brtt.com>), providing many of the methods commonly used for single event

location (Pavlis et al., 2004). The GENLOC library is based on the LOCSAT algorithm (Bratt and Bache, 1988), which originated from the nuclear monitoring program, and is also considered a well tested and robust location program. The program accepts any combination of arrival times and slowness vectors, and can utilize seismic phases, with predicted travel times and/or slowness vectors, provided by the user. It is applicable at any scale from local to global networks, and replaces the azimuth data by slowness vectors. This is done in order to avoid some of the intrinsic problems of azimuth data used in many location algorithms, in which at high velocities or close to the source, azimuth becomes unstable. The location search is done by the standard Gauss-Newton Method (Lee and Stewart, 1981), originally suggested by Geiger (1910), and uses a linear approximation to relate perturbation in the hypocenter parameters to the data. Error handling is done based on Pavlis (1986), in which the total error is a linear sum of the main three types of source-errors: measurement error, modeling error, and non-linearity. The ***relocate*** program has a comfortable database interface, allowing the examination of various velocity models.

Velocity model

Several velocity models were used at the GII to create the earthquake bulletin, and to the best of our knowledge, in the past decade, many of the events were located based on the velocity model of Feigin and Shapira (1994). In addition, several geographical subsets of the data were relocated, as part of high-resolution studies (e.g., Alderson et al. 2003, Hofstetter et al., 2012, Wetzler et al., 2014, for the Dead Sea Basin; Shamir et al., 2003, Hofstetter et al. 2003 for the gulf of Eilat; Navon 2011 for Sea of Galilee), and several velocity models were used and developed (i.e., Gitterman et al., 2005; Mechie et al., 2009) as part of those studies. We examined many of these models (including the one of Feigin and Shapira (1994), which we name JStar), trying to find the most reliable velocity model, providing the most stable solution with the smallest errors. Gitterman et al. (2005) provided the most recent work, treating the entire region of the DSF, using a set of controlled explosions recorded by all network stations, searching for a velocity model with the best fit to the known origin times and locations. We chose to relocate the seismic catalog here by local velocity model of Gitterman et al., (2005), named here GITT05. We also used the IASP91 velocity model (Kennett and Engdahl, 1991) as a standard reference, which for the purpose of

local-scale seismicity can be treated almost as a single layer model, providing stable solutions. However, while for Southern California, IASP91 is a reasonable approximation, due to the high percentage of igneous rocks at relatively shallow depths (Mooney and Weaver, 1989), in the DSF region there are higher percentage of sedimentary rocks with lower seismic velocities at the shallow crust (up to ~5km depth). This means that although the IASP91 locations are more stable, they are over estimating the depth, since the higher velocities at shallow depths "push" the solution deeper into the crust.

Results

Our new relocated catalog includes 15,181 events, which are 95.7% of the original catalog, remaining after the removal of the poorly constrained locations. Figure 3 shows a) a map view of the relocated events (Figure 3a), and b) depth histograms of different subsets of the events (Figure 3b). It seems that, on average, the original locations (Figure 2) and the new relocations (Figure 3) show quite a similar horizontal pattern, meaning that at least the epicenters did not shift significantly by modifications in the velocity models, and in the location algorithms. The main story of the new relocations is in the new depth distribution presented in Figure $3b_1$, showing that events are located significantly deeper than the original locations, and having an average vertical shift of ~10 km (using the median). While in the original catalog ~90% of the events were located within the upper 5 km of the crust, after the relocation they are distributed down to 35 km depth, showing an active seismogenic zone with a peak activity at 15 km depth; these numbers are similar for both velocity models, presented by gray (IASP91) and black (GITT05) bars of Figure 3b. Figure 3 also shows the coverage area of the seismic network, marking the area of the seismic network boundaries (dashed line) in which within it, locations are well constrained (***In-Network***), and beyond it, locations are poorly constrained (***Off-Network***). Examining Figure 3b we see that while within the coverage area of the seismic network we obtain a reasonable depth distribution (Figure $3b_2$), as expected for the seismotectonic settings of the DSF zone, epicenters located north (Figure $3b_3$) and south (Figure $3b_4$) of the seismic network coverage area have a large number of shallow events. We claim that events located out of the boundaries of the seismic network are poorly constrained due to the lack of azimuthal station coverage.

There were no consistent error estimations of the original relocations, and the majority of events were not assigned an error at all, even in respect to the arrival times, estimated manually by seismic analysts. Therefore, error analysis was done only for the *relocate* algorithm, comparing between the different velocity models. Figure 4 shows the comparison between the IASP91 and the GITT05 velocity models, showing significantly smaller vertical (Figure 4c) and horizontal (Figure 4a, b) errors for the latter, summarized also by statistical measures in Table 1. As both solutions share the same algorithm and differ only in their velocity models, we interpret the smaller errors as better overall fit of the GITT05 velocity model, and its corresponding locations as our preferred solution. Figure 4 also shows that for the GITT05 velocity model, the error estimations in the horizontal axes are fairly similar to the errors on the vertical axis, with a peak distribution around an error of 0.2-0.25 km. In the case of the IASP91 velocity model, while for the horizontal axes the error peak distribution is around 0.45-0.5 km, the vertical error distribution shows larger errors, with a peak around 0.75 km. Moreover, beyond the statistics, GITT05 velocity model is a more reasonable model than IASP91, accounting for the lower seismic velocities at the upper sedimentary layers of the study area (e.g., Ginzburg and Ben-Avraham, 1997; Hofstetter et al., 2000; Gitterman et al., 2005; Laske and Weber, 2008).

Statistical analysis

Up to this point we examined the relocated events, showing that the main effect is in achieving a reliable depth distribution of the event locations. We will now examine the horizontal shift of the relocated epicenters from their original locations. On the one hand, we would like to check that there is no horizontal bias due to the relocation algorithm, velocity model and / or station distribution; on the other hand, horizontal shifts with preferred orientation might reflect a problem in the original locations that was corrected by the new relocations. In Figure 5, we compare the horizontal-azimuth shift, measured between the original locations and the new relocations, within 20° slices, for the two velocity models: GITT05, and IASP91. In Figures $5a_1$ and $5b_1$, we count the number of horizontal shifts in each slice, showing quite homogeneous distribution, with no preferred orientation. However, this is not the complete picture, it does not consider the magnitude of these shifts (measured by horizontal distance). This is done in Figures $5a_2$ and $5b_2$, in which for each slice we

calculate the median horizontal shift. It is done for all the events (dark blue), and then also for three subsets: ***In-Network*** (magenta), ***Off-Network*** North (light blue) and ***Off-Network*** South (green). While for ***In-Network*** events we see almost homogeneous median shifts, for both velocity models, beyond the coverage area the pattern becomes more heterogeneous: a) for the northern events the median shifts seem to be randomly distributed, and b) for the southern events we see preferred orientation in a sub parallel S-N direction. The latter is also seen in Figure 5c, emphasizing the main difference between the relocations obtained by the two velocity models. For the GITT05 velocity model, the depth relocations, shifts the events on a S-N axis, with no clear preference, due to the similarity to the JStar velocity model. However, for the IASP91 velocity model, the seismic velocities at shallow depths are significantly higher, resulting in a strong effect, in which all those events that were pushed down in the relocations had to be moved further away from the recording stations; that is to say that events were shifted to the south, compensating for the faster ray path travel time. The overall effect of the median horizontal shifts is seen by the dark blue line, which averages all the above considerations. It seems that similar to the error analysis, the horizontal shifts analysis is also showing that the GITT05 local velocity model provides a more stable solution than the IASP91 global velocity model, with less significant bias due the event-station distribution.

Discussion

Earthquake locations and velocity models

We have separated the events into two main regions: a) ***In-Network*** - within the coverage area and b) ***Off-Network*** - beyond the coverage area of the stations; this was done since the latter has an embedded lack of information, leading to large uncertainties in the resulting locations (Gary Pavlis, Personal Communication). However, even with these large uncertainties, we have shown that with the ***relocate*** program we obtain more reasonable locations, not only within the coverage area, but also beyond it. Comparing between the two velocity models: GITT05 and IASP91, we see quite consistent and expected characteristics, in which: a) velocity models with high velocity layers will push the epicenters deeper, b) for ***Off-Network*** events, the faster the seismic velocity of a layer, the further away from the stations they would be

located, and c) error estimation of the relocations, generated by both velocity models, show that at least in our case, errors obtained from local GITT05 velocity model relocations, are lower than the global IASP91 errors. Still, locations beyond the coverage area, especially in the southern tip should be taken with a grain of salt (Gary Pavlis, Personal Communications), since location estimations in this type of situation are simply poorly constrained (Pavlis et al., 2004). Reality might be somewhere in-between these two models, but the error bounds, calculated by the ***relocate*** program, are not representing the problem well enough, in order to resolve this issue with more certainty. For those areas, a more focused research should be done (if possible), only for the periods in which there was a better coverage of stations. This will provide better locations for those periods, and might be used as an additional constraint when locating events originating in the same region, at times of sparse station-coverage.

Seismogenic Depth along the Dead Sea Fault

The main benefit obtained by the relocations, is that we could now examine seismogenic zones along the DSF and CFS systems. An example to this is presented in Figure 6, showing the distribution of the seismicity in a narrow N-S trending band, along the DSF. The 0.75 quantile curve (continuous gray) marks the depth boundary of 75% of the events; meaning that the majority of the events do not go beyond that depth. This curve is compared to an estimation of the thermal profile along the DSF, obtained by Shalev et al. (2013) by interpolating heat flux measurements. The seisomogenic depth is estimated according to the 300-350º temperature contours, indicating the maximum temperatures for brittle failure (Ranalli, 1995; Jaupart and Mareschal, 2010). Here we show that the new relocations provide fairly similar estimation of the seismogenic depth, as suggested by Shalev et al. (2013), reflecting for example, deep seismicity at the cold crust of the Dead Sea Basin (Aldersons et al. 2003; Shamir 2006), and shallow seismicity at the hot crust beneath the Sea of Galilee (Navon, 2011). Furthermore, our seismogenic depth profile is better constrained, showing additional features and depth anomalies that were not seen in Shalev et al. (2013), due to interpolation limitations of the heat-flow measurements, used to construct the siesmogenic depth profile of Shalev et al. (2013).

The correlation between the seismogenic depth and the heat flow was observed and discussed, regarding other tectonic regions. For example, in Southern California, Magistrale (2002) has shown that the seismogenic depth (defined by the 0.95

quantile) is strongly heat-flow and lithology dependent, exhibiting deeper seismogenic depth for lower heat flows, and for more Mafic compositions. Hong and Menke (2006) focused on the San Jacinto fault zone showing that the 0.95 quantile corresponds to the 400º: colder crust at the NW of the fault correlated with deeper seismicity, and warmer crust at the SE of the fault correlated with shallower seismicity. Their definition for the seismogenic depth (0.95 quantile) is presented in Figure 6 (dashed gray), better capturing the overall seismicity, and approximately correlated to the 400º contour.

Bonner et al. (2003) have shown a more complex picture of the heat-flow to seismogenic-depth relation. Analyzing all California, and defining the seismogenic depth according to the 0.99 quantile, some of the regions have shown correlation to the 450º contour, and some of the lower heat-flow provinces (<50 mW/m2) have shown correlation to the 260º contour. Bonner hypothesized that other factors such as stress regime and strain rate contribute to these differences. More detailed work on these issues are yet to come, once we compile our results with specific areas, in which, previous high resolution studies have been made in the past.

Conclusions

We applied the *relocate* program, which is a robust single event location algorithm, in order to reprocess the arrival-times of the past 30 years in the vicinity of Israel and the Dead Sea Fault. The result is a revised seismic catalogue for the region of Israel, with a significant contribution to the depths of the seismicity in the region, showing a more reasonable depth distribution in the region. This catalogue should be the basis for future, more elaborated relocation methods e.g., HYPODD (Waldhauser and Ellsworth, 2000). From all the velocity models tested in this study, the one by Gitterman et al. (2005) has shown the smallest errors, and provided the most reasonable and reliable locations.

For the relocated catalogue we separated between the events within the coverage area of the network, and beyond it, due to the significant difference in their associated uncertainties. For ***In-Network*** events, the location-uncertainty is small, and is reflected also by the small horizontal shifts, with no preferred orientation. For ***Off-Network*** events, the location-uncertainty is larger and is reflected by the larger horizontal shifts. For the southern events, originating at the Gulf of Eilat, the

horizontal shifts are showing a clear preferred N-S orientation, which is more pronounced to the south, meaning that more events were shifted further away from the recording stations.

We show that the seismicity could be applied to define the seismogenic zone of the DSF, fitting nicely to the seismogenic depths derived from the heat flux interpolation of Shalev et al. (2013). Moreover, while the Shalev profile is interpolated also in regions with hardly any measurements, we have higher resolution, obtaining a more detailed and accurate profile of the seismogenic zone.

We suggest replacing the current seismic bulletin with our new relocated bulletin, so that it could serve as an initial, more reliable reference for future seismological studies of the region. The new catalogue will be soon available for download, together with GIS layers and Google Earth layers for the convenience of the users, in the website of the Geological Survey of Israel, GSI (<https://www.gsi.gov.il>).

We have completed here a fundamental step in our research objective to improve our estimation of the capable tectonic sources in the region of Israel; improved locations set the underlying foundation required for achieving this goal.

Acknowledgements We thank Batya Reich, Andrey Polozov, Lea Feldman, Veronic Avrirav, and David Kadosh of the Division of Seismology for their assistance in gathering the data and information, presented in this study.

References

Aldersons, F., Ben-Avraham, Z., Hofstetter, A., Kissling, E., and Al-Yazjeen, T., 2003, Lower-crustal strength under the Dead Sea basin from local earthquake data and rheological modeling: Earth and Planetary Science Letters, v. 214, no. 1-2, p. 129–142, doi: 10.1016/s0012-821x(03)00381-9.

Ben-Avraham, Z., Ginzburg, A., Makris, J., and Eppelbaum, L., 2002, Crustal structure of the Levant basin, eastern Mediterranean: Tectonophysics, v. 346, no. 1-2, p. 23–43.

Bonner, J.L., Blackwell, D.D., and Herrin, E.T., 2003, Thermal constraints on earthquake depths in California: Bulletin of the Seismological Society of America, v. 93, no. 6, p. 2333–2354.

Bratt, S.R., and Bache, T.C., 1988, Locating events with a sparse network of regional arrays: Bulletin of the Seismological Society of America, v. 78 , no. 2 , p. 780–798.

Brothers, D.S., Driscoll, N.W., Kent, G.M., Harding, a. J., Babcock, J.M., and Baskin, R.L., 2009, Tectonic evolution of the Salton Sea inferred from seismic reflection data: Nature Geoscience, v. 2, no. 8, p. 581–584, doi: 10.1038/ngeo590.

Feigin, G., and Shapira, A., 1994, A unified crustal model for calculating travel times of seismic waves across the Israel Seismic Network: IPRG Rep. Z, v. 1.

Garfunkel, Z., 2014, Lateral motion and deformation along the Dead Sea Transform, *in* Garfunkel, Z., Ben-Avraham, Z., and Kagan, E. eds., Dead Sea Transform Fault System: Reviews, Modern Approaches in Solid Earth Sciences, Springer Netherlands, Dordrecht, p. 109 – 145.

Garfunkel, Z., Zak, I., and Freund, R., 1981, Active faultind in the Dead Sea rift: Tectonophysics, v. 80, p. 1–26.

Geiger, L., 1910, Herdbestimmung bei Erdbeben aus den Ankunftszeiten: Nachrichten von der Gesellschaft der Wissenschaften zu Göttingen, Mathematisch-Physikalische Klasse, v. 1910, p. 331–349.

Ginzburg, A., and Ben-Avraham, Z., 1997, A seismic refraction study of the north basin of the Dead Sea, Israel: Geophysical Research Letters, v. 24, no. 16, p. 2063–2066.

Ginzburg, A., Makris, J., Fuchs, K., Perathoner, B., and Prodehl, C., 1979, Detailed structure of the crust and upper mantle along the Jordan-Dead Sea Rift: Journal of Geophysical Research: Solid Earth, v. 84, no. B10, p. 5605–5612, doi: 10.1029/JB084iB10p05605.

Gitterman, Y., Pinsky, V., Shapira, A., Ergin, M., Kalafat, D., Gurbuz, G., and Solomi, K., 2005, IMPROVEMENT IN DETECTION, LOCATION, AND IDENTIFICATION OF SMALL EVENTS THROUGH JOINT DATA ANALYSIS BY SEISMIC STATIONS IN THE MIDDLE EAST/EASTERN MEDITERRANEAN REGION:.

Grall, C., Henry, P., Tezcan, D., Mercier de Lepinay, B., Becel, a., Geli, L., Rudkiewicz, J.-L., Zitter, T., and Harmegnies, F., 2012, Heat flow in the Sea of Marmara Central Basin: Possible implications for the tectonic evolution of the North Anatolian fault: Geology, v. 40, no. 1, p. 3–6, doi: 10.1130/G32192.1.

Hofstetter, A., Dorbath, C., and Calò, M., 2012, Crustal structure of the Dead Sea basin from local earthquake tomography: Geophysical Journal International, v. 189, no. 1, p. 554–568.

Hofstetter, A., Dorbath, C., Rybakov, M., and Goldshmidt, V., 2000, Crustal and upper mantle structure across the Dead Sea rift and Israel from teleseismic P-wave tomography and gravity data: Tectonophysics, v. 327, no. 1-2, p. 37–59.

Hofstetter, A., Eck, T. Van, and Shapira, A., 1996, Seismic activity along fault branches of the Dead Sea-Jordan transform system: the Carmel-Tirtza fault system: Tectonophysics, v. 267, p. 317–330.

Hofstetter, a, Thio, H.K., and Shamir, G., 2003, Source mechanism of the 22 / 11 / 1995 Gulf of Aqaba earthquake and its: , p. 99–114.

Hong, T.K., and Menke, W., 2006, Tomographic investigation of the wear along the San Jacinto fault, southern California: Physics of the Earth and Planetary Interiors, v. 155, no. 3-4, p. 236–248, doi: 10.1016/j.pepi.2005.12.005.

Jaupart, C., and Mareschal, J.-C., 2010, Heat generation and transport in the Earth: Cambridge university press.

Kennett, B.L.N., and Engdahl, E.R., 1991, Traveltimes for global earthquake location and phase identification: Geophysical Journal International, v. 105, no. 2, p. 429–465, doi: 10.1111/j.1365-246X.1991.tb06724.x.

Koulakov, I., and Sobolev, S. V, 2006, Moho depth and three-dimensional P and S structure of the crust and uppermost mantle in the Eastern Mediterranean and Middle East derived from tomographic inversion of local ISC data: Geophysical Journal International, v. 164, no. 1, p. 218–235, doi: 10.1111/j.1365-246x.2005.02791.x.

Lachenbruch, A.H., Sass, J.H., and Galanis, S.P., 1985, Heat flow in southernmost California and the origin of the Salton Trough: Journal of Geophysical Research, v. 90, p. 6709, doi: 10.1029/JB090iB08p06709.

Laske, G., and Weber, M., 2008, Lithosphere structure across the Dead Sea Transform as constrained by Rayleigh waves observed during the DESERT experiment: Geophysical Journal International, v. 173, no. 2, p. 593–610, doi: 10.1111/j.1365-246X.2008.03749.x.

Lay, T., and Wallace, T.C., 1995, Modern global seismology: Academic Press, San Diego.

Lee, W.H.K., and Stewart, S.W., 1981, Principles and applications of microearthquake networks: Academic Press.

Lyakhovsky, V., Ben-Avraham, Z., and Achmon, M., 1994, The origin of the Dead Sea rift: Tectonophysics, v. 240, no. 1-4, p. 29–43, doi: 10.1016/0040-1951(94)90262-3.

Magistrale, H., 2002, Relative contributions of crustal temperature and composition to controlling the depth of earthquakes in Southern California: Geophysical Research Letters, v. 29, no. 10, p. 2–5, doi: 10.1029/2001GL014375.

Makris, J., Abraham, Z.B., Behle, A., Ginzburg, A., Giese, P., Steinmetz, L., Whitmarsh, R.B., and Eleftheriou, S., 1983, Seismic refraction profiles between Cyprus and Israel and their interpretation: Geophysical Journal International, v.

75, no. 3, p. 575–591, doi: 10.1111/j.1365-246X.1983.tb05000.x.

Mechie, J., Abu-Ayyash, K., Ben-Avraham, Z., El-Kelani, R., Qabbani, I., and Weber, M., 2009, Crustal structure of the southern Dead Sea basin derived from project DESIRE wide-angle seismic data: Geophysical Journal International, v. 178, no. 1, p. 457–478, doi: 10.1111/j.1365-246X.2009.04161.x.

Mooney, W.D., and Weaver, C.S., 1989, Regional crustal structure and tectonics of the Pacific coastal states; California, Oregon, and Washington: Geological Society of America Memoirs, v. 172, p. 129–162.

Navon, H., 2011, Microseismic characterization of Lake Kinneret basin: MSc Thesis: Tel-Aviv University.

Palano, M., Imprescia, P., and Gresta, S., 2013, Current stress and strain-rate fields across the Dead Sea Fault System: Constraints from seismological data and GPS observations: Earth and Planetary Science Letters, v. 369-370, p. 305–316, doi: 10.1016/j.epsl.2013.03.043.

Pavlis, G.L., 1986, Appraising earthquake hypocenter location errors: A complete, practical approach for single-event locations: Bulletin of the Seismological Society of America, v. 76, no. 6, p. 1699–1717.

Pavlis, G.L., Vernon, F., Harvey, D., and Quinlan, D., 2004, The generalized earthquake-location (GENLOC) package: An earthquake-location library: Computers and Geosciences, v. 30, no. 9-10, p. 1079–1091, doi: 10.1016/j.cageo.2004.06.010.

Plenefisch, T., and Bonjer, K.-P., 1997, The stress field in the Rhine Graben area inferred from earthquake focal mechanisms and estimation of frictional parameters: Tectonophysics, v. 275, no. 1–3, p. 71–97, doi: http://dx.doi.org/10.1016/S0040-1951(97)00016-4.

Polozov, A., and Pinsky, V., 2004, New software for seismic network and array data processing and joint seismological data base. First year report GII 546/075/04. Prepared for the Ministry of National Infrastructures:.

Quennell, A.M., 1956, Tectonics of the Dead Sea rift: Congreso Geologico Internacional, 20th sesion, Asociacion de Servicios Geologicos Africanos, p. 358–405.

Ranalli, G., 1995, Rheology of the Earth: Springer Science & Business Media.

Ron, H., 1987, Deformation along the Yammuneh, The restraining bend of the Dead Sea Transform: Paleomagnetic data and kinematic implications: Tectonics, v. 6, no. 5, p. 653, doi: 10.1029/TC006i005p00653.

Rybakov, M., Goldshmidt, V., and Rotstein, Y., 1997, New regional gravity and magnetic maps of the Levant: Geophysical Research …, v. 24, no. 1, p. 33–36.

Sadeh, M., Hamiel, Y., Ziv, A., Bock, Y., Fang, P., and Wdowinski, S., 2012, Crustal deformation along the Dead Sea Transform and the Carmel Fault inferred from 12 years of GPS measurements: Journal of Geophysical Research, v. 117, no. B8, p. 1–14, doi: 10.1029/2012JB009241.

Sato, T., Kasahara, J., Taymaz, T., Ito, M., Kamimura, A., Hayakawa, T., and Tan, O., 2004, A study of microearthquake seismicity and focal mechanisms within the Sea of Marmara (NW Turkey) using ocean bottom seismometers (OBSs): Tectonophysics, v. 391, no. 1-4 SPEC.ISS., p. 303–314, doi: 10.1016/j.tecto.2004.07.018.

Segev, A., and Rybakov, M., 2011, History of faulting and magmatism in the Galilee (Israel) and across the Levant continental margin inferred from potential field data: Journal of Geodynamics, v. 51, no. 4, p. 264–284, doi: 10.1016/j.jog.2010.10.001.

Segev, A., Rybakov, M., Lyakhovsky, V., Hofstetter, A., Tibor, G., Goldshmidt, V., and Ben-Avraham, Z., 2006, The structure, isostasy and gravity field of the Levant continental margin and the southeast Mediterranean area: Tectonophysics, v. 425, no. 1-4, p. 137–157, doi: 10.1016/j.tecto.2006.07.010.

Shalev, E., Lyakhovsky, V., Weinstein, Y., and Ben-Avraham, Z., 2013, The thermal structure of Israel and the Dead Sea Fault: Tectonophysics, v. 602, p. 69–77, doi: 10.1016/j.tecto.2012.09.011.

Shamir, G., Baer, G., and Hofstetter, a, 2003, Three-dimensional elastic earthquake modelling based on integrated seismological and InSAR data : the M w = 7 . 2 Nuweiba earthquake , gulf of Elat / Aqaba 1995 November: Transform, p. 731–744.

Shapira, A., and Hofstetter, R., 2007, EARTHQUAKE HAZARD ASSESSMENTS FOR BUILDING CODES:.

Shearer, P.M., Hauksson, E., and Lin, G.Q., 2005, Southern california hypocenter relocation with waveform cross-correlation, part 2: Results using source-specific station terms and cluster analysis: Bulletin of the Seismological Society of America, v. 95, no. 3, p. 904–915, doi: 10.1785/01200401168.

Sibson, R.H., 1982, Fault zone models, heat flow, and the depth distribution of earthquakes in the continental crust of the United States: B. Seismol. Soc. Am., v. 72, no. 1, p. 151–163.

De Vicente, G., Cloetingh, S., Muñoz-Martín, a., Olaiz, a., Stich, D., Vegas, R., Galindo-Zaldívar, J., and Fernández-Lozano, J., 2008, Inversion of moment tensor focal mechanisms for active stresses around the microcontinent Iberia: Tectonic implications: Tectonics, v. 27, no. 1, p. n/a–n/a, doi: 10.1029/2006TC002093.

Waldhauser, F., and Ellsworth, W.L., 2000, A double-difference earthquake location algorithm: Method and application to the northern Hayward fault, California:

Bulletin of the Seismological Society of America, v. 90, no. 6, p. 1353–1368.

Weber, M., Ayyash, K.A., Abueladas, A., Agnon, A., Al-Amoush, H., Babeyko, A., Bartov, Y., Baumann, M., Ben-Avraham, Z., Bock, G., Bribach, J., El-Kelani, R., Forster, A., Forster, H.J., et al., 2004, The crustal structure of the Dead Sea Transform: Geophysical Journal International, v. 156, no. 3, p. 655–681, doi: 10.1111/j.1365-246X.2004.02143.x.

Wetzler, N., Sagy, A., and Marco, S., 2014, The Association of Micro-earthquake Clusters with Mapped Faults in the Dead Sea Basin: Journal of Geophysical Research, v. 119, no. 11, p. 1–19, doi: 10.1002/2013JB010877.

Zaliapin, I., and Ben-Zion, Y., 2013, Earthquake clusters in southern California I: Identification and stability: Journal of Geophysical Research: Solid Earth, , no. 8004, p. n/a–n/a, doi: 10.1002/jgrb.50179.

Tables

	Location (JStar)				Relocation (IASP91)				Relocation (GITT05)			
	Events	Err x	Err y	Err z	Events	Err x	Err y	Err z	Events	Err x	Err y	Err z
All	15856	8.4	4	6	15150	0.77	1.05	1.3	15181	0.7	1	1.2
In-Network	6576	2.3	1.3	2.2	5909	0.44	0.56	0.78	6223	0.43	0.5	0.8
Off-Network-N	1447	6.5	3.2	3.2	1783	0.71	0.86	1.14	1528	0.78	1.05	1.3
Off-Network-S	7833	135	17	30	7454	1.47	1.83	2.35	7430	1.39	1.74	2.27

Table 1: Median values of locations and relocations misfits (measured in km) calculated for a) the initial locations, and for the Antelope relocations using b) IASP91 global velocity model, and c) GITT05 local velocity model (Gitterman et al., 2005). Errors are presented in kilometers for four distribution types: ***All*** events, ***In-Network*** events, ***Off-Network-N*** events and the ***Off-Network-S*** events. The area of the ***In-Network*** events is presented by the rectangle in Figure 3.

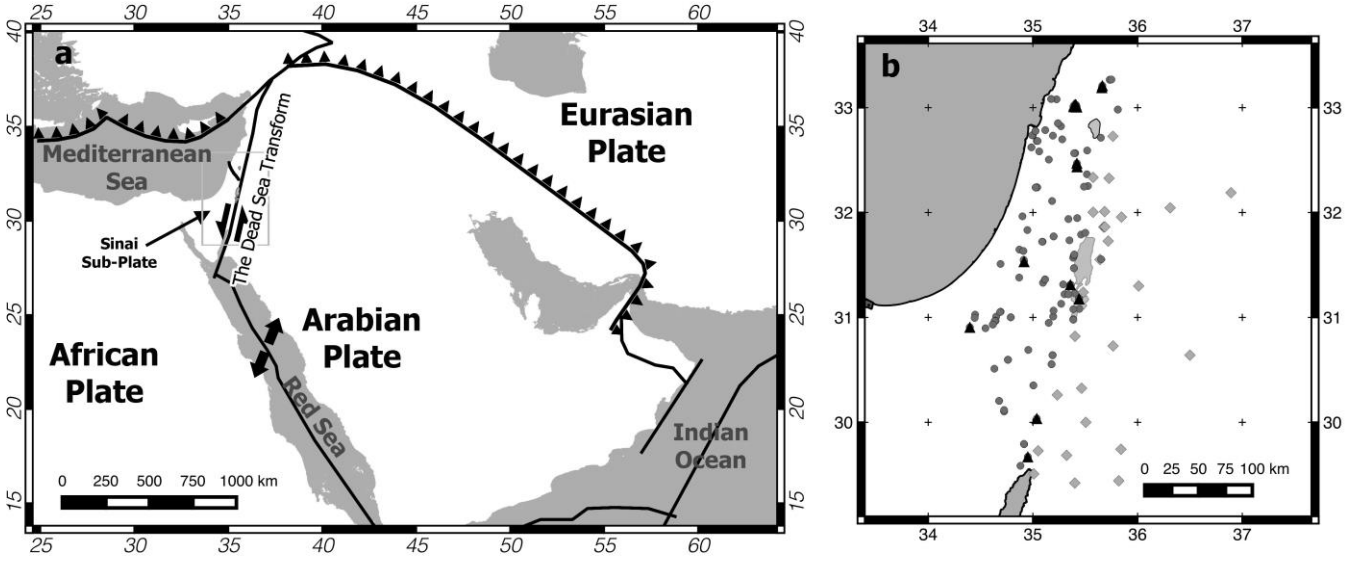

Figure 1: a) Map of the the Middle East, including the regional major fault systems (black lines). The regional tectonic plate configuration is presented along with the relative horizontal slip motions (black arrows). The research area is marked by the gray rectangle. b) The regional seismic stations that were operational within the period of 1985 – 2015, including those of the Israel Seismic Network (dark gray circles– short period, black triangles - broadband), and those of the Jordanian Seismic Observatory (light gray diamonds).

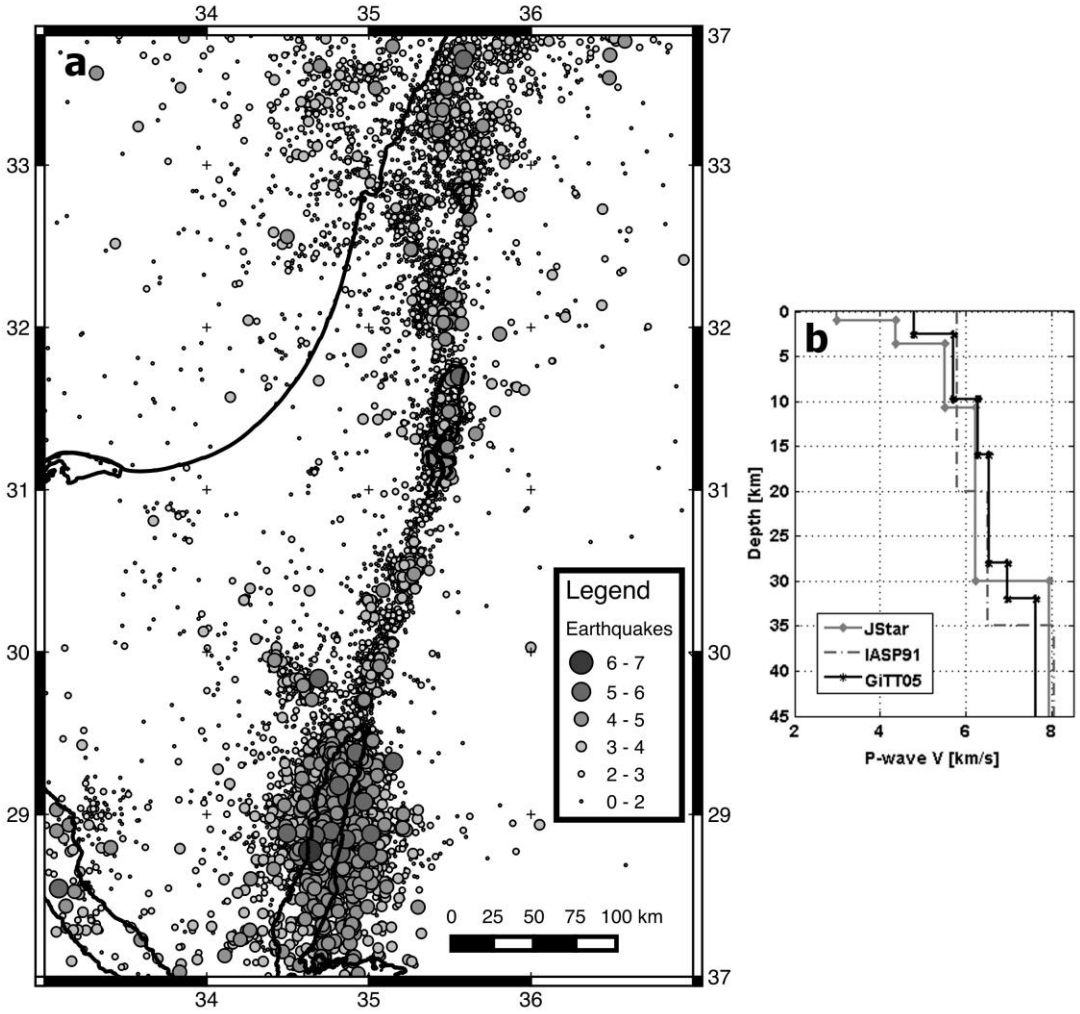

Figure 2: a) The earthquake catalog recorded by the GII between 1985 and 2015, having a total of 15856 events. Filled circles show the new locations of the seismic events, with their size scaled by magnitude. b) The seismic P-wave velocity models applied for the region. The initial location was obtained by JStar's software model (line with diamonds) and for the relocations we used the velocity model of Gitterman et al. (2005) (GITT05 - black line); the IASP91 global crustal model is given here for reference (dashed line).

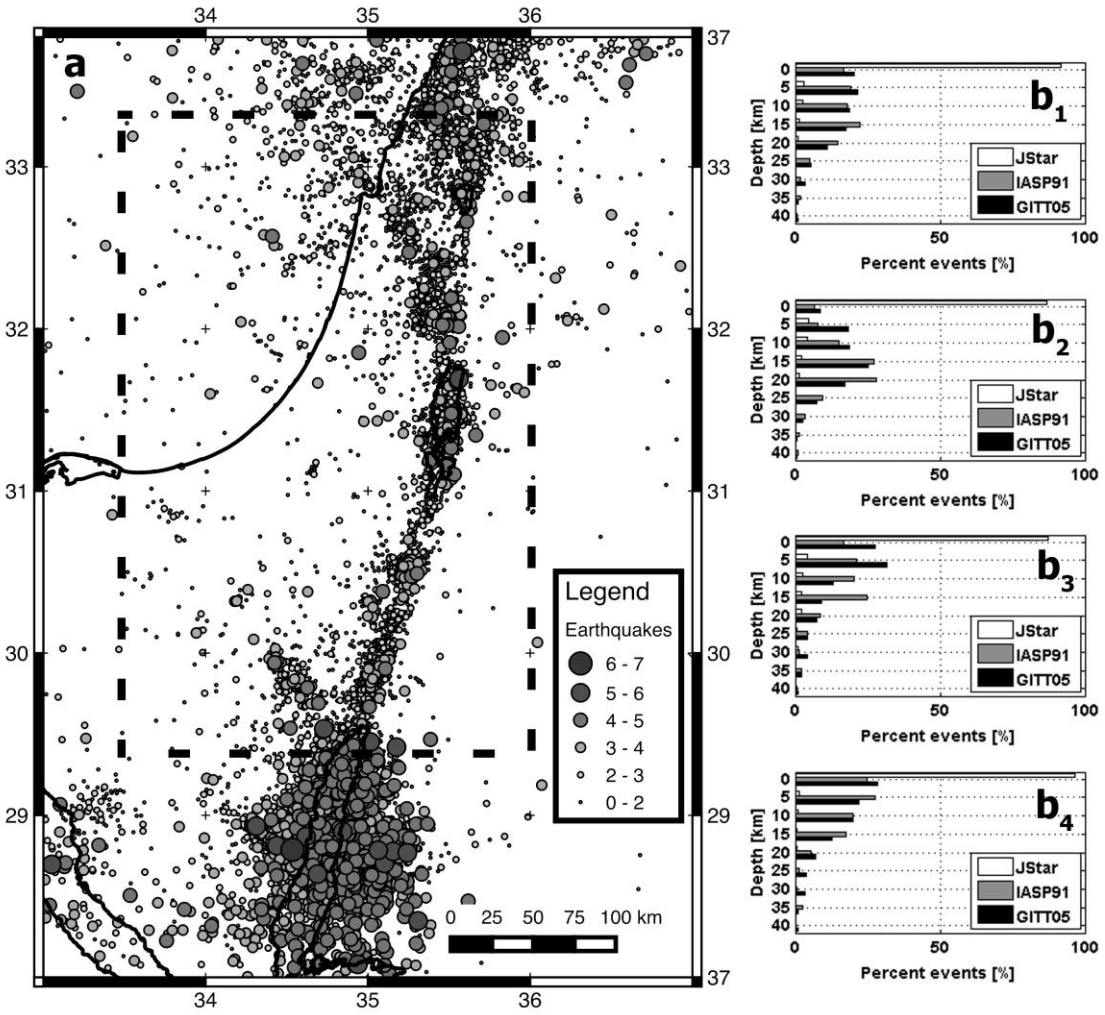

Figure 3: The relocated catalog, based on the P and S arrivals recorded by the GII between 1985 and 2015, with a total of 15181 events. Filled circles show the new locations of the seismic events, with their size scaled by magnitude. The ***coverage area*** of the seismic network is marked by the black dashed rectangle; beyond this area, locations are poorly constrained**.** b) Depth histograms of the original (white- 'Catalog'), relocated events using Gitterman et al. (2005) velocity model (GITT05 - black), and relocated events using IASP91 velocity model (gray), of four catalog types: b1) all events, b2) events within the coverage area **(*In-Network*)**, b3) ***Off-Network*** North events, and b4) ***Off-Network*** South events.

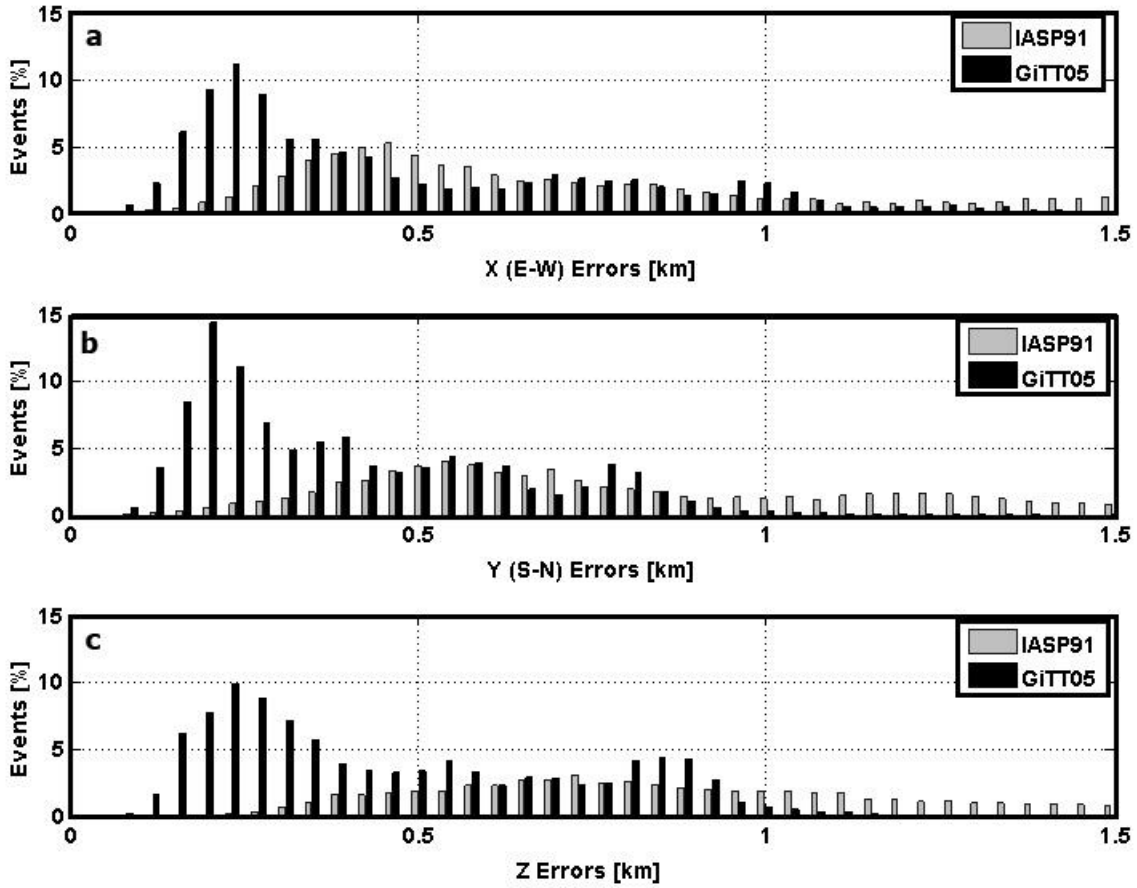

Figure 4: Location errors for the two velocity models: IASP91 in gray histograms, and GITT05 (following Gitterman et al., 2005) in black, for three geographical axes: a) X-axis (East-West), b) Y-axis (North-South), and c) Vertical axis .

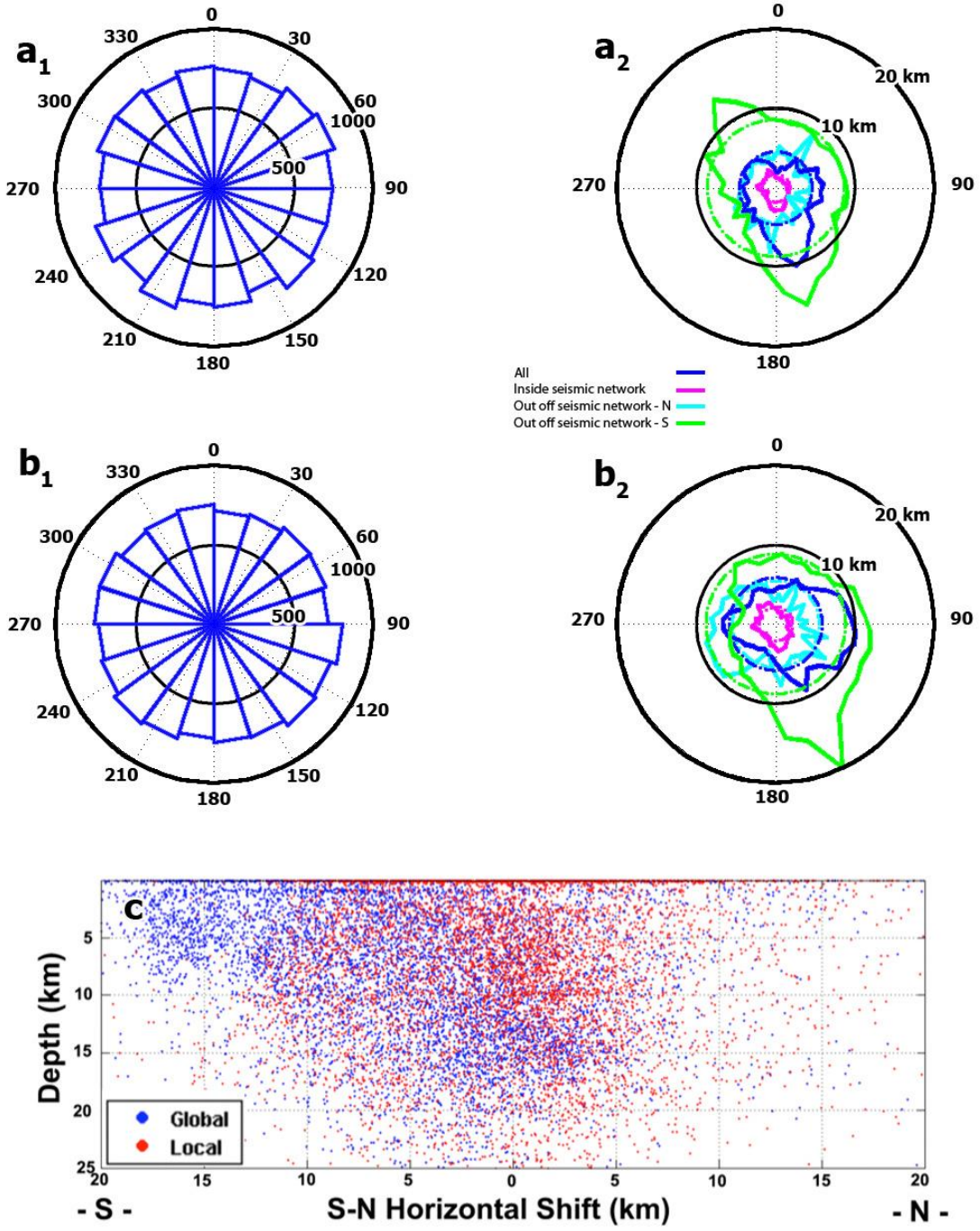
a1
0
30
60
90
120
150
180
210
240
270
300
330
500
1000
a2
20 km
10 km
All
Inside seismic network
Out off seismic network - N
Out off seismic network - S
b1
b2
c
Depth (km)
Global
Local
- S -
S-N Horizontal Shift (km)
- N -

Figure 5: The horizontal location shifts for two velocity models are presented, using the JStar original locations as the reference for these shifts. The upper row (a1 and a2) are for the relocations obtained by the velocity model of Gitterman et al. (2005), and the middle row (b1 and b2) are for the relocations obtained by IASP91. The rose diagrams, a1 and b1, show the azimuthal shifts measured from the earthquake initial location to the new location; the radius of the 20° slices mark the number of events within the slice, and the contours are of the number of events**.** Note that both velocity models show homogeneous azimuthal distribution for all the relocated events. The polar diagrams, a2 and b2, show the median shifts for each direction (in meters) for several subsets of the data: all events (blue), in-grid events - located within the coverage area (magenta); off-grid events - located north of the coverage area (light blue), and off-grid events - located south of the coverage area (green). Dashed circles present the total medians shift: a2) 4617, 1779, 4382 and 8157 meters for Gitterman 2005 velocity model, and b2) 5916, 2161, 5521, and 8918 for IASP91, respectfully; c) Cross section emphasizing the S-N horizontal shifts of the off-grid events - located south of the coverage area. The shifts are seen down to 25km depth, for two velocity models: IASP91 ("Global" blue), and Gitterman et al. 2005 ("Local" red). While the shifts of the local model are scattered around the zero, with no clear preference, the shifts of the global model show a strong shift to the south, related to the significantly higher wave velocity at the shallow subsurface.

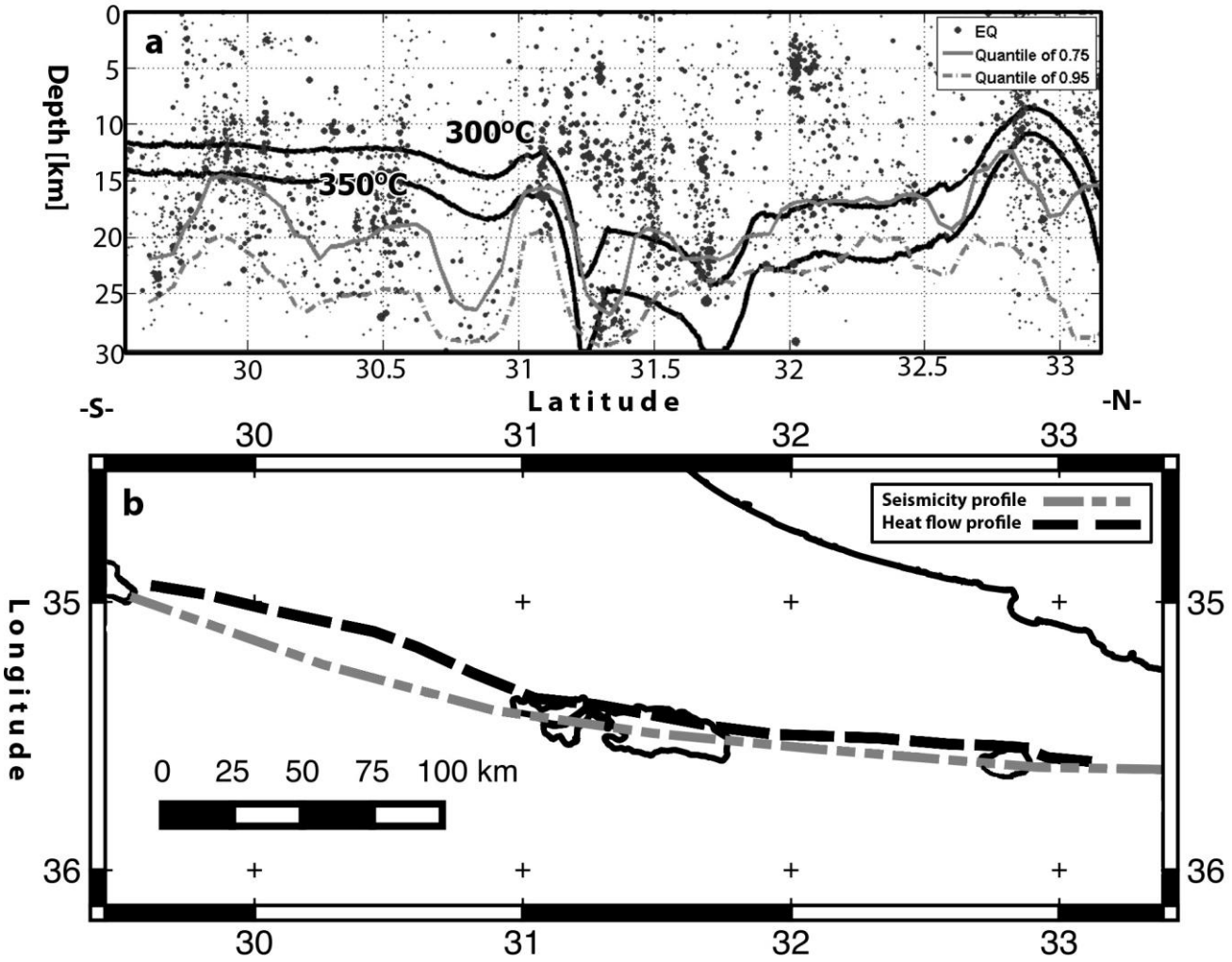

Figure 6: The seismogenic zone along the DSF; the dashed gray line in (b), is plotted by gray lines in (a) according to a moving quantile of 0.75 (solid), and 0.95 (dashed), applying a window of 10 km (~N-S axis) by 15 km (~E-W), in 5 km intervals. The two black lines are the temperature contours of 300 °C and 350 °C calculated by Shalev et al. (2013) along the DSF, and marked by the black dashed line in (b).

Defining and mapping capable tectonic sources for seismic hazard estimation in Israel: general analysis and specific focus for nuclear power plants in Israel

Appendix

Accepted for publication in Seismological Research Letters

The earthquake activity of Israel - Revisiting 30 years of local and regional seismic record along the Dead Sea Transform

Nadav Wetzler[1,2] and Ittai Kurzon[1]

(1) Geological Survey of Israel, Jerusalem, Israel

(2) Department of Geosciences, Tel Aviv University, Tel Aviv, Israel

Ministry of National Infrastructures, Energy and Water Resources Grants:

#212-17-003 and #214-11-010

The earthquake activity of Israel - Revisiting 30 years of local and regional seismic record along the Dead Sea Transform

Nadav Wetzler[1,2] and Ittai Kurzon[1]

(1) Geological Survey of Israel, Jerusalem, Israel

(2) Department of Geosciences, Tel Aviv University, Tel Aviv, Israel

Abstract

More than 15,000 seismic events were recorded by the Israel Seismic Network (ISN) during the past 30 years, at the vicinity of the Dead Sea Fault (DSF) zone. During those years locations were obtained using several velocity models, which resulted in inconsistent locations. In addition, we found that seismicity is biased to very shallow depth estimations that do not match other estimations of more localized studies in the region. This study is focused on improving the regional earthquake catalog using robust single event location software (within the Antelope software), based on two seismic velocity models: a) a local model (Gitterman et. al., 2005), and b) a global model (Kennett and Engdahl, 1991). The relocated events show more reasonable depth distributions, in accordance with the seismo-tectonic settings of the region, and the local velocity model shows smaller location errors than the global velocity model, suggesting better convergence of the location solutions. We also demonstrate and analyze the difference in the event-station distribution, showing location effects of a sparse network, in which the main effect is seen for the focal depths: events located out of the network coverage tend to obtain a focal depth shallower than events located within the network coverage. The depth cross-section along the DSF zone, within the

boundaries of this study, presents a good correlation with previous estimation of the boundaries of the seismogenic zone, obtained by heat-flow analysis. The relocated earthquake catalogue is regarded as the new initial robust locations of the seismic bulletin of the ISN, and considered as the basis for future studies and for more elaborated relocations; it is open to the public and can be downloaded from the Geological Survey of Israel (GSI) website at: <https://www.gsi.gov.il>.

Introduction

Large-scale observations of spatial patterns of earthquake hypocenters show that seismicity is located mainly along plate boundaries (Lay and Wallace, 1995). For smaller scales, such as for regional or local seismic activity, this seismo-tectonic relation is more obscured, and requires higher resolutions of the sub-plate boundaries and fault systems, and an accurate earthquake locations (e.g. Hauksson and Shearer, 2005; Hauksson et al., 2012). Therefore, as we try to extract more information from seismicity patterns, we soon face the issue of how precise is the earthquake catalogue we are examining.

One of the main issues in characterizing fault systems is to determine the seismogenic zones, in which strains are accommodated mainly by brittle failure. The seismogenic zone is affected by many variables; from regional and local stress fields (e.g., Plenefisch and Bonjer, 1997; de Vicente et al., 2008; Palano et al., 2013), through lateral and vertical lithological changes (Aldersons et al., 2003; Brothers et al., 2009), to heat flux ascending from the mantle (Lachenbruch et al., 1985; Grall et al., 2012; Shalev et al., 2013). The base of the seismogenic zone is theoretically determined from the brittle-ductile transition and is commonly set to 300 -- 350°C (e.g., Shalev et al., 2013). Therefore in order to properly determine the observed seismogenic zone (e.g., Sibson, 1982) it is crucial that the seismic depths within an earthquake catalogue are well constrained. Typically, focal depth and origin time have lower accuracy than the epicenter, since they are less sensitive to the geometry of the network, and therefore are highly sensitive to the applied velocity model (e.g. Husen and Hardebeck, 2010; Bondár and Storchak, 2011). Besides the general issue of improving earthquake locations (e.g., Allam et al., 2014), the issue of improving their

focal depths is very significant for the characterization of active seismogenic zones. Similar to the general expectation that the epicenters will fall in close proximity to surface fault traces, we would expect that the hypocenters will have depth distribution reflecting the lithology, fault structure, and other measures observed in the examined region (e.g., heat flux).

The Israeli Seismic Network (ISN) had been established in 1983 (Shapira and Hofstetter, 2007), and was expanded and upgraded several times, following the technological developments in seismometry, gradually including more three-component, broadband, seismic sensors since 1996. The network monitors the research area (Figure 1b), providing specifically good coverage of the Dead Sea Fault (DSF) system and the Carmel Fault System (CFS). Over the past 30 years several velocity models have been applied to locate the seismic activity, some of the models have been inserted into *JStar*, the local software, and several single-event location algorithms have been applied; naturally, this has lead to inconsistent seismic locations. The current data-processing procedure includes an initial automatic detection and location of seismic events, shortly followed by a) analyst review and fine tuning of the P and S detections, b) relocation and c) magnitude estimation. In the process of a current upgrade of the system we reviewed the seismic catalogue recorded over the years, and found that there is a bias to very shallow depth estimations, which do not match other observations that are known from more localized studies in the region (Hofstetter et al., 1996; Aldersons et al., 2003; Hofstetter et al., 2012; Wetzler et al., 2014), and the observations seen in other similar seismo-tectonic regions (e.g., Sato et al., 2004; Shearer et al., 2005; Zaliapin and Ben-Zion, 2013).

Our first order solution was to revisit the locations of the entire seismic catalogue, assuming that the P and S picks are valid, using a single robust velocity model of the

region, and applying a high quality location algorithm. To achieve this goal we applied the relocate algorithm and the GENLOC library, of the Antelope package (<https://www.brtt.com>). The results and initial analysis provided in the following text establish a renewed earthquake catalogue, with better locations, and a more reasonable depth distribution.

Geological Background

The crustal structure of Israel is characterized by southeast declining Moho boundary, sub-parallel to the Israeli coastline, associated with a transition zone between the relatively thin intermediate crust of the Eastern Mediterranean Sea (20 km depth) and the thicker crust of Jordan (32 km depth) (Segev et al., 2006). This structure was retrieved by the compilation of several studies including inversion of teleseismic P waves (Hofstetter et al., 2000), refraction profiles (Ginzburg et al., 1979; Makris et al., 1983; Ben-Avraham et al., 2002; Weber et al., 2004; Koulakov and Sobolev, 2006), and gravity and magnetic maps (Rybakov et al., 1997; Segev et al., 2006).

Israel is also located close to a large fault system, the Dead Sea Transform (DST), extending from the southern Red Sea spreading center to the northern zone of plate convergence in southern Turkey, a distance of ~1,000 km, defining the plate boundary between the Arabian and African-Sinai plates (Figure 1). The left-lateral slip motion along the DST has accommodated horizontal displacement of ~100 km (Quennell, 1956; Garfunkel et al., 1981; Garfunkel, 2014), in a mean slip motion of ~5 mm/year (Sadeh et al., 2012) since the Early Miocene. The tectonic activity along the DST has formed a series of deep basins: the Gulf of Elat (Aqaba), the Sea of Galilee and the Dead Sea Basin (Figure 1b), which is the largest and deepest of these basins. The

Carmel-Gilboa-Faria fault system (Figure 1a) is an additional fault system, located in northern Israel, and striking NW-SE, diagonally to the DST (Figure 1a), and it has been suggested that it precedes the DST, developing during the Senonian (Segev and Rybakov, 2011).

The ongoing tectonic activity along the major regional fault system over the past 30 years is demonstrated by the seismicity presented in Figure 2. The seismicity pattern highlights the plate boundaries showing localized seismicity along the DST, and the northern branching of the transform fault system (Ron, 1987; Lyakhovsky et al., 1994).

The strongest recorded event in the last 160 years was the 1995, Mw 7.2 (Figure 2) earthquake, that was followed by 6 months of intense aftershock activity, and was interpreted as a strike-slip fault (Baer et al., 2008). Paleoseismological studies demonstrate that moderate to large magnitude (M > 7) earthquakes occurred along the DST (Shapira et al., 1993; Marco et al., 1996; Marco and Agnon, 2005; Agnon et al., 2006; Wetzler et al., 2010; Lazar et al., 2010). In addition, historical records attest to the occurrence of moderate to strong earthquakes along the DST, which caused extensive damage to historical settlements, which was observed at damaged structures throughout the region (Marco, 2008).

Previous seismological studies have demonstrated a relatively deep seismogenic activity, located in the Dead Sea area, indicating focal depths down to ~25 km (Aldersons et al., 2003; Hofstetter et al., 2012; Wetzler et al., 2014). These observations, as well as surface heat flux measurements indicate a cold crust, characterized by deep brittle failure (Shalev et al., 2013).

Dataset and Data Processing

Seismological dataset

We reprocessed the seismic activity of the Dead Sea Fault region, from January 1985 to February 2015, within a geographic rectangle of 33-37 longitude, and 28-34 latitude. This dataset includes 15,856 earthquakes (Figure 2), in magnitudes of $0.5 \leq M_d \leq 7.2$, collected by the Geophysical Institute of Israel (GII). The GII has been monitoring the seismic activity in the region during the past 30 years, using the ISN (Figure 1b) and consisting of a total of ~ 140 seismic stations. Over these years many of these stations were modified: some were de-activated, others upgraded to 3-component digital seismometers, and some are still operating similar to their original settings. Since the ISN includes various types of seismometers, the sampling rates in the seismic stations vary between 20 sps for the older stations to 100 sps for the modern ones. The current data acquisition system, operated and maintained by the Division of Seismology of the GII, incorporates the ISN stations, two CTBT stations (Comprehensive Nuclear Test-Ban Treaty), and several CNF stations (Cooperating National Facility). A significantly smaller percentage of the data is incorporated from other regional networks: a) GE, Geophone global network of GFZ, b) JSO, the Jordanian Seismic Observatory, and c) CQ, the seismic network of Cyprus.

Data processing

The earthquake bulletin includes the origin location of the seismic events, their origin time, and the P- and S- wave arrival times reviewed and refined by GII's analysts. In addition, it contains the error estimations of the locations, based on the picking errors of the arrival times, assigned by the analysts, and errors due to the

location algorithm and to the 1-D velocity model (Polozov and Pinsky, 2004). We regarded the arrival times as the most reliable measure we have, and we have examined the remaining components, mainly focusing on the velocity model used for the relocations.

Relocation method

We applied the ***relocate*** program of the Antelope software. The program is an end-user interface to the Generalized Location (GENLOC) Library of Antelope software (<www.brtt.com>), providing many of the methods commonly used for single event location (Pavlis et al., 2004). The GENLOC library is based on the LOCSAT algorithm (Bratt and Bache, 1988), which originated from the nuclear monitoring program, and is also considered a well tested and robust location program. The program accepts any combination of arrival times and slowness vectors, and can utilize seismic phases, with predicted travel times and/or slowness vectors, provided by the user. It is applicable at any scale from local to global networks, and replaces the azimuth data by slowness vectors. This is done in order to avoid some of the intrinsic problems of azimuth data used in many location algorithms, in which at high velocities or close to the source, azimuth becomes unstable. The location search is carried out according to the standard Gauss-Newton Method (Lee and Stewart, 1981), originally suggested by Geiger (1910), and uses a linear approximation to relate perturbation in the hypocenter parameters to the data. Error handling is done based on Pavlis (1986), in which the total error is a linear sum of the main three types of source-errors: measurement error, modeling error, and non-linearity.

Velocity model

Several velocity models were used at the GII to create the earthquake bulletin,

and to the best of our knowledge, in the past decade, many of the events were located based on the velocity model of Feigin and Shapira (1994). In addition, several geographical subsets of the data were relocated, as part of high-resolution studies (e.g., Alderson et al. 2003, Hofstetter et al., 2012, Wetzler et al., 2014, for the Dead Sea Basin; Shamir et al., 2003, Hofstetter et al. 2003 for the gulf of Eilat; Navon 2011 for Sea of Galilee), and several velocity models were used and developed (i.e., Gitterman et al., 2005; Mechie et al., 2009) as part of those studies. We examined many of these models (including the one of Feigin and Shapira (1994), which we name *JStar*), trying to find the most reliable velocity model, providing the most stable solution with the smallest errors. A basic comparison of all of these models was carried out at the initial stage of this study, and is further presented and discussed in the Appendix. The outcome of this basic relocation analysis was that we should focus on two models: a) the local / regional velocity model of Gitterman et al., (2005), named here GITT05 and b) the global / regional IASP91 velocity model (Kennett and Engdahl, 1991). Gitterman et al. (2005) provided the most comprehensive work done in the region, treating the entire area of the DSF, using a set of controlled explosions recorded by all network stations, and searching for a velocity model with the best fit to the known origin times and locations. The IASP91 velocity model is considered for several reasons: a) it is a regional / global velocity model, and the dimensions of the area examined in this study is of a regional scale - 6° N-S and 4° E-W, b) some of the areas within the study area, such as the Gulf of Eilat and southwest Jordan have igneous lithology that could be approximated by the IASP91 velocity model, and c) for the purpose of local-scale seismicity it can be treated almost as a single layer model, providing stable reference solutions for the locations obtained by using the GITT05 velocity model. However, while for Southern California, IASP91 is a

reasonable approximation, due to the high percentage of igneous rocks at relatively shallow depths (Mooney and Weaver, 1989), in the DSF region there is a higher percentage of sedimentary rocks with lower seismic velocities at the shallow crust (down to ~5km depth). This means that although the IASP91 locations are more stable in general, on a local scale and at the more sediment-oriented regions, locations are overestimating the depth, since the higher velocities at shallow depths "push" the solution deeper into the crust.

Results

Our new relocated catalog includes 15,181 events (Figure 3a), which are 95.7% of the original catalog remaining after the removal of the poorly constrained locations. It seems that, on average, the original locations (Figure 2) and the relocations (Figure 3a) show quite a similar horizontal pattern, meaning that at least the epicenters did not shift significantly by modifications in the velocity models and in the location algorithms. The main story of the relocated events is in the new depth distribution presented in Figure $3b_1$, showing that events are located significantly deeper than the original locations, and having an average vertical shift of ~10 km (using the median). While in the original catalog ~90% of the events were located within the upper 5 km of the crust, after the relocation they are distributed down to 35 km depth, showing an active seismogenic zone with a peak activity at 15 km depth (Figure $3b_1$); these numbers are similar for both velocity models, presented by the dashed (IASP91) and black (GITT05) bars of Figure 3b. Figure 3 also shows the coverage area of the seismic network, marking the area of the seismic network boundaries (dashed line) in which within it, locations are well constrained (In-Network), and beyond it, locations are poorly constrained (Off-Network). By examining Figure 3b we see that while

within the coverage area of the seismic network we obtain a reasonable depth distribution as expected from the seismotectonic settings of the DSF zone (Figure $3b_2$), epicenters located north (Figure $3b_3$) and south (Figure $3b_4$) of the seismic network coverage area have a large number of shallow events. We claim that events located out of the boundaries of the seismic network are poorly constrained due to the lack of azimuthal station coverage.

There were no consistent error estimations of the original relocations, and the majority of events were not assigned an error at all, even with respect to the arrival times, estimated manually by seismic analysts. Therefore, error analysis was done only for the relocations obtained by the *relocate* algorithm, comparing the two velocity models: GITT05 and IASP91. Figure 4 shows the horizontal (X and Y) and vertical (Z) error estimation for both velocity models, and for three main event datasets: All, In-Network and Off-Network. Note, that although each of the axes and each of the datasets show different error estimations, both velocity models have quite similar error histograms for each of the subplots examined in Figure 4. The similarity in error estimation is emphasized by the values of the absolute difference between the medians of both models, $|dMed.|$, presented within the legends of the subplots. As expected, the error estimations for the Off-Network subsets are much higher than the In-Network subsets, also manifested by the mean medians (black solid line) presented in the histograms. In most of the subplots, the histograms show slightly higher bars of the lower range errors, for the GITT05, suggesting a slightly better model. This observation is manifested in Table 1, concluding that, in the overall of the error statistical analysis, GITT05 shows slightly smaller errors than IASP91. This statistical preference supports the more fundamental reason to adopt GITT05 as the preferred velocity model: the GITT05 velocity model is a more reasonable model than IASP91,

accounting for the lower seismic velocities at the upper sedimentary layers of the study area (e.g., Ginzburg and Ben-Avraham, 1997; Hofstetter et al., 2000; Gitterman et al., 2005; Laske and Weber, 2008).

Statistical analysis

Up to this point we have examined the relocated events, showing that the main effect is in achieving a reliable depth distribution of the event locations. We will now examine the horizontal shift of the relocated epicenters from their original locations. On the one hand, we would like to check that there is no horizontal bias due to the relocation algorithm, velocity model and / or station distribution; on the other hand, horizontal shifts with preferred orientation might reflect a problem in the original locations that was corrected by the relocations. In Figure 5 we compare the horizontal-azimuth shift, measured between the original locations and the relocations, within 20° slices, for the two velocity models: GITT05, and IASP91. We count the number of horizontal shifts in each slice (Figures $5a_1$ and $5b_1$), showing a rather homogeneous distribution, with no preferred orientation. However, this is not the complete picture, since it does not consider the magnitude of these shifts (measured by horizontal distance). This is done in Figures $5a_2$ and $5b_2$, in which for each slice we calculate the median horizontal shift. This is done for all the events (dark blue), and also for three subsets: In-Network (magenta), Off-Network North (light blue) and Off-Network South (green). While for the In-Network events we see almost homogeneous median shifts (for both velocity models), beyond the coverage area the pattern becomes more heterogeneous: a) for the northern events the median shifts seem to be randomly distributed, and b) for the southern events we see preferred orientation in a sub-parallel S-N direction. The latter is also seen in Figure 5c,

emphasizing the main difference between the relocations obtained by the two velocity models. For the GITT05 velocity model, the depth relocations shift the events on a S-N axis, with no clear preference, due to the similarity to the JStar velocity model. However, for the IASP91 velocity model, the seismic velocities at shallow depths are significantly higher, resulting in a strong effect, in which all those events that were pushed down in the relocations had to be moved further away from the recording stations; that is to say, events were shifted to the south, compensating for the faster ray path travel time. The overall effect of the median horizontal shifts is seen by the dark blue line, which averages all the above considerations. It seems that, similar to the error analysis, the horizontal shifts analysis also shows that the GITT05 local / regional velocity model provides a more stable solution than the IASP91 regional / global velocity model, with less significant bias due the event-station distribution.

Discussion

Earthquake locations and velocity models

We have separated the events into two main regions: a) In-Network -- within the coverage area, and b) Off-Network -- beyond the coverage area of the stations; this was done since the latter has an embedded lack of information, leading to large uncertainties in the resulting locations (Gary Pavlis, Personal Communication). However, even with these large uncertainties, we have shown that with the relocate program we obtain more reasonable locations, not only within the coverage area, but also beyond it. Comparing between the two velocity models, GITT05 and IASP91, we see quite consistent and expected characteristics, in which a) velocity models with high velocity layers will push the epicenters deeper, b) for Off-Network events, the faster the seismic velocity of a layer, the further away from the stations they would be

located, and c) error estimation of the relocations, generated by both velocity models, show that at least in our case, errors obtained from local / regional GITT05 velocity model relocations are slightly lower than the regional / global IASP91 errors. Still, locations beyond the coverage area, especially in the southern tip should be taken with a grain of salt (Gary Pavlis, Personal Communications), since location estimations in this type of situation are simply poorly constrained (Pavlis et al., 2004). Reality might be somewhere in-between these two models, but the error bounds, calculated by the relocate program, do not represent the problem well enough, in order to resolve this issue with more certainty. For those areas, a more focused research should be carried out (if possible), only for the periods in which there was a better coverage of stations. This will provide better locations for those periods, and might be used as an additional constraint when locating events originating in the same region, at times of sparse station-coverage.

Seismogenic Depth along the Dead Sea Fault

The main benefit obtained by the relocations is that we could now examine seismogenic zones along the major fault systems. An example is presented in Figure 6, showing the distribution of the seismicity in a narrow N-S trending band, along the DSF. The 0.75 quantile curve (continuous gray) marks the depth boundary of 75% of the events, meaning that the majority of the events do not go beyond that depth. This curve is compared to an estimation of the thermal profile along the DSF, obtained by Shalev et al. (2013) by interpolating heat flux measurements. The seismogenic depth is estimated according to the 300-350º temperature contours, indicating the maximum temperatures for brittle failure (Ranalli, 1995; Jaupart and Mareschal, 2010). Here we show that the relocations provide fairly similar estimation of the seismogenic depth, as suggested by Shalev et al. (2013), reflecting for example, deep seismicity at the

cold crust of the Dead Sea Basin (Aldersons et al., 2003; Shamir, 2006), and shallow seismicity at the hot crust beneath the Sea of Galilee (Navon, 2011). Furthermore, our seismogenic depth profile is better constrained, showing additional features and depth anomalies that were not seen in Shalev et al. (2013), due to interpolation limitations of the heat-flow measurements, used to construct the seismogenic depth profile of Shalev et al. (2013).

The correlation between the seismogenic depth and the heat flow was observed and discussed, regarding other tectonic regions. For example, in Southern California, Magistrale (2002) has shown that the seismogenic depth (defined by the 0.95 quantile) is strongly heat-flow and lithology dependent, exhibiting deeper seismogenic depth for lower heat flows, and for more Mafic compositions. Hong and Hong and Menke (2006) focused on the San Jacinto fault zone showing that the 0.95 quantile corresponds to the 400º: colder crust at the NW of the fault correlated with deeper seismicity, and warmer crust at the SE of the fault correlated with shallower seismicity. Their definition for the seismogenic depth (0.95 quantile) is presented in Figure 6 (dashed gray), better capturing the overall seismicity, and approximately correlated to the 400º contour.

Bonner et al. (2003) have shown a more complex picture of the heat-flow to seismogenic-depth relation. Analyzing all California, and defining the seismogenic depth according to the 0.99 quantile, some of the regions have shown correlation to the 450º contour, and some of the lower heat-flow provinces (<50 mW/m2) have shown correlation to the 260º contour. Bonner hypothesized that other factors such as stress regime and strain rate contribute to these differences. More detailed work on these issues are yet to come, once we compile our results with specific areas, in which, previous high resolution studies have been made in the past.

Conclusions

We applied the *relocate* program, which is a robust single event location algorithm, in order to reprocess the arrival-times of the past 30 years in the vicinity of Israel and the Dead Sea Fault. The result is a revised seismic catalogue for the region of Israel, with a significant contribution to the depths of the seismicity, showing a more reasonable depth distribution in the region. This catalogue should be the basis for future, more elaborated relocation methods e.g., HYPODD (Waldhauser and Ellsworth, 2000). From all the velocity models tested in this study, the one by Gitterman et al. (2005) has shown relatively low errors, and provided the most reasonable and reliable locations.

For the relocated catalogue we separated between the events within the coverage area of the network, and beyond it, due to the significant difference in their associated uncertainties. For In-Network events, the location-uncertainty is small, and is reflected also by the small horizontal shifts, with no preferred orientation. For Off-Network events, the location-uncertainty is larger and is reflected by the larger horizontal shifts. For the southern events, originating at the Gulf of Elat, the horizontal shifts are showing a clear preferred N-S orientation, which is more pronounced to the south, meaning that more events were shifted further away from the recording stations.

We show that the seismicity could be applied to define the seismogenic zone of the DSF, fitting nicely to the seismogenic depths derived from the heat flux interpolation of Shalev et al. (2013). Moreover, while the Shalev profile is interpolated also in regions with hardly any measurements, we have higher resolution, obtaining a more detailed and accurate profile of the seismogenic zone.

We suggest replacing the current seismic bulletin with our new relocated bulletin, so that it could serve as an initial, more reliable reference for future seismological studies of the region. The new catalogue can be downloaded, together with GIS layers and Google Earth layers for the convenience of the users, in the website of the Division of Seismology (<https://seis.gii.co.il>) and in the website of the Geological Survey of Israel, GSI (<https://www.gsi.gov.il>).

Acknowledgements We thank Batya Reich, Andrey Polozov, Lea Feldman, Veronic Avrirav, and David Kadosh of the Division of Seismology for their assistance in gathering the data and information, presented in this study. This research was supported by the Israel Science Foundation (grant ISF 929/10) and by the Ministry of National Infrastructures, Energy and Water Resources (Grant numbers: 212-17-003, and 214-11-010).

354 **References**

355 Agnon, A., Migowski, C., and Marco, S., 2006, Interclust breccia layers in laminated
356 sequences reviewed: recorders of paleo-earthquakes: Geological Society of
357 America, v. 401, p. 195–214.

358 Aldersons, F., Ben-Avraham, Z., Hofstetter, A., Kissling, E., and Al-Yazjeen, T.,
359 2003, Lower-crustal strength under the Dead Sea basin from local earthquake
360 data and rheological modeling: Earth and Planetary Science Letters, v. 214, no.
361 1-2, p. 129–142, doi: 10.1016/s0012-821x(03)00381-9.

362 Allam, a. a., Ben-Zion, Y., Kurzon, I., and Vernon, F., 2014, Seismic velocity
363 structure in the Hot Springs and Trifurcation areas of the San Jacinto fault zone,
364 California, from double-difference tomography: Geophysical Journal
365 International, v. 198, no. 2, p. 978–999, doi: 10.1093/gji/ggu176.

366 Baer, G., Funning, G.J., Shamir, G., and Wright, T.J., 2008, The 1995 November 22,
367 Mw 7.2 gulf of elat earthquake cycle revisited: Geophysical Journal
368 International, v. 175, p. 1040–1054, doi: 10.1111/j.1365-246X.2008.03901.x.

369 Ben-Avraham, Z., Ginzburg, A., Makris, J., and Eppelbaum, L., 2002, Crustal
370 structure of the Levant basin, eastern Mediterranean: Tectonophysics, v. 346, no.
371 1-2, p. 23–43.

372 Bondár, I., and Storchak, D., 2011, Improved location procedures at the International
373 Seismological Centre: Geophysical Journal International, v. 186, no. 3, p. 1220–
374 1244, doi: 10.1111/j.1365-246X.2011.05107.x.

375 Bonner, J.L., Blackwell, D.D., and Herrin, E.T., 2003, Thermal constraints on
376 earthquake depths in California: Bulletin of the Seismological Society of
377 America, v. 93, no. 6, p. 2333–2354.

378 Bratt, S.R., and Bache, T.C., 1988, Locating events with a sparse network of regional
379 arrays: Bulletin of the Seismological Society of America , v. 78 , no. 2 , p. 780–
380 798.

381 Brothers, D.S., Driscoll, N.W., Kent, G.M., Harding, a. J., Babcock, J.M., and Baskin,
382 R.L., 2009, Tectonic evolution of the Salton Sea inferred from seismic reflection
383 data: Nature Geoscience, v. 2, no. 8, p. 581–584, doi: 10.1038/ngeo590.

384 Feigin, G., and Shapira, A., 1994, A unified crustal model for calculating travel times
385 of seismic waves across the Israel Seismic Network: IPRG Rep. Z, v. 1.

386 Garfunkel, Z., 2014, Lat motion and deformation along the Dead Sea Transform, *in*
387 Garfunkel, Z., Ben-Avraham, Z., and Kagan, E.J. eds., Dead Sea Transform
388 Fault System: Reviews, Modern Approaches in Solid Earth Sciences, Springer
389 Netherlands, Dordrecht, p. 109 – 145.

390 Garfunkel, Z., Zak, I., and Freund, R., 1981, Active faultind in the Dead Sea rift:

391 Tectonophysics, v. 80, p. 1–26.

392 Geiger, L., 1910, Herdbestimmung bei Erdbeben aus den Ankunftszeiten:
393 Nachrichten von der Gesellschaft der Wissenschaften zu Göttingen,
394 Mathematisch-Physikalische Klasse, v. 1910, p. 331–349.

395 Ginzburg, A., and Ben-Avraham, Z., 1997, A seismic refraction study of the north
396 basin of the Dead Sea, Israel: Geophysical Research Letters, v. 24, no. 16, p.
397 2063–2066.

398 Ginzburg, A., Makris, J., Fuchs, K., Perathoner, B., and Prodehl, C., 1979, Detailed
399 structure of the crust and upper mantle along the Jordan-Dead Sea Rift: Journal
400 of Geophysical Research: Solid Earth, v. 84, no. B10, p. 5605–5612, doi:
401 10.1029/JB084iB10p05605.

402 Gitterman, Y., Pinsky, V., Shapira, A., Ergin, M., Kalafat, D., Gurbuz, G., and
403 Solomi, K., 2005, Improvement in detection, location, and identification of small
404 events through joint data analysis by seismic stations in the Middle East/Eastern
405 Mediterranean region:.

406 Grall, C., Henry, P., Tezcan, D., Mercier de Lepinay, B., Becel, a., Geli, L.,
407 Rudkiewicz, J.-L., Zitter, T., and Harmegnies, F., 2012, Heat flow in the Sea of
408 Marmara Central Basin: Possible implications for the tectonic evolution of the
409 North Anatolian fault: Geology, v. 40, no. 1, p. 3–6, doi: 10.1130/G32192.1.

410 Hauksson, E., and Shearer, P.M., 2005, Southern California hypocenter relocation
411 with waveform cross-correlation, Part 1: Results using the double-difference
412 method: Bulletin of the Seismological Society of America, v. 95, no. 3, p. 896–
413 903, doi: 10.1785/0120040167.

414 Hauksson, E., Yang, W., and Shearer, P.M., 2012, Waveform Relocated Earthquake
415 Catalog for Southern California (1981 to June 2011): Bulletin of the
416 Seismological Society of America, v. 102, no. 5, p. 2239–2244, doi:
417 10.1785/0120120010.

418 Hofstetter, A., Dorbath, C., and Calò, M., 2012, Crustal structure of the Dead Sea
419 basin from local earthquake tomography: Geophysical Journal International, v.
420 189, no. 1, p. 554–568.

421 Hofstetter, A., Dorbath, C., Rybakov, M., and Goldshmidt, V., 2000, Crustal and
422 upper mantle structure across the Dead Sea rift and Israel from teleseismic P-
423 wave tomography and gravity data: Tectonophysics, v. 327, no. 1-2, p. 37–59.

424 Hofstetter, A., Eck, T. Van, and Shapira, A., 1996, Seismic activity along fault
425 branches of the Dead Sea-Jordan transform system: the Carmel-Tirtza fault
426 system: Tectonophysics, v. 267, p. 317–330.

427 Hofstetter, A., Thio, H.K., and Shamir, G., 2003, Source mechanism of the 22 / 11 /
428 1995 Gulf of Aqaba earthquake and its: , p. 99–114.

Hong, T.K., and Menke, W., 2006, Tomographic investigation of the wear along the San Jacinto fault, southern California: Physics of the Earth and Planetary Interiors, v. 155, no. 3-4, p. 236–248, doi: 10.1016/j.pepi.2005.12.005.

Husen, S., and Hardebeck, J.L., 2010, Earthquake location accuracy: Community Online Resource for Statistical Seismicity Analysis, v. 10.

Jaupart, C., and Mareschal, J.-C., 2010, Heat generation and transport in the Earth: Cambridge university press.

Kennett, B.L.N., and Engdahl, E.R., 1991, Traveltimes for global earthquake location and phase identification: Geophysical Journal International, v. 105, no. 2, p. 429–465, doi: 10.1111/j.1365-246X.1991.tb06724.x.

Koulakov, I., and Sobolev, S. V., 2006, Moho depth and three-dimensional P and S structure of the crust and uppermost mantle in the Eastern Mediterranean and Middle East derived from tomographic inversion of local ISC data: Geophysical Journal International, v. 164, no. 1, p. 218–235, doi: 10.1111/j.1365-246x.2005.02791.x.

Lachenbruch, A.H., Sass, J.H., and Galanis, S.P., 1985, Heat flow in southernmost California and the origin of the Salton Trough: Journal of Geophysical Research, v. 90, p. 6709, doi: 10.1029/JB090iB08p06709.

Laske, G., and Weber, M., 2008, Lithosphere structure across the Dead Sea Transform as constrained by Rayleigh waves observed during the DESERT experiment: Geophysical Journal International, v. 173, no. 2, p. 593–610, doi: 10.1111/j.1365-246X.2008.03749.x.

Lay, T., and Wallace, T.C., 1995, Modern global seismology: Academic Press, San Diego.

Lazar, M., Ben-Avraham, Z., Marco, S., Garfunkel, Z., Porat, N., and Ben-Avraham, Z., 2010, Is the Jericho Escarpment a Tectonic or a Geomorphological Feature? Active Faulting and Paleoseismic Trenching: The Journal of Geology, v. 118, no. 3, p. 261–276, doi: 10.1086/651504.

Lee, W.H.K., and Stewart, S.W., 1981, Principles and applications of microearthquake networks: Academic Press.

Lyakhovsky, V., Ben-Avraham, Z., and Achmon, M., 1994, The origin of the Dead Sea rift: Tectonophysics, v. 240, no. 1-4, p. 29–43, doi: 10.1016/0040-1951(94)90262-3.

Magistrale, H., 2002, Relative contributions of crustal temperature and composition to controlling the depth of earthquakes in Southern California: Geophysical Research Letters, v. 29, no. 10, p. 2–5, doi: 10.1029/2001GL014375.

Makris, J., Abraham, Z.B., Behle, A., Ginzburg, A., Giese, P., Steinmetz, L., Whitmarsh, R.B., and Eleftheriou, S., 1983, Seismic refraction profiles between

Cyprus and Israel and their interpretation: Geophysical Journal International, v. 75, no. 3, p. 575–591, doi: 10.1111/j.1365-246X.1983.tb05000.x.

Marco, S., 2008, Recognition of earthquake-related damage in archaeological sites: Examples from the Dead Sea fault zone: Tectonophysics, v. 453, no. 1-4, p. 148–156.

Marco, S., and Agnon, A., 2005, High-resolution stratigraphy reveals repeated earthquake faulting in the Masada Fault Zone, Dead Sea Transform: Tectonophysics, v. 408, no. 1-4, p. 101–112.

Marco, S., Stein, M., Agnon, A., and Ron, H., 1996, Long-term earthquake clustering: A 50,000-year paleoseismic record in the Dead Sea Graben: Journal of Geophysical Research, v. 101, no. B3, p. 6179–6191.

Mechie, J., Abu-Ayyash, K., Ben-Avraham, Z., El-Kelani, R., Qabbani, I., and Weber, M., 2009, Crustal structure of the southern Dead Sea basin derived from project DESIRE wide-angle seismic data: Geophysical Journal International, v. 178, no. 1, p. 457–478, doi: 10.1111/j.1365-246X.2009.04161.x.

Mooney, W.D., and Weaver, C.S., 1989, Regional crustal structure and tectonics of the Pacific coastal states; California, Oregon, and Washington: Geological Society of America Memoirs, v. 172, p. 129–162.

Navon, H., 2011, Microseismic characterization of Lake Kinneret basin: MSc Thesis: Tel-Aviv University.

Palano, M., Imprescia, P., and Gresta, S., 2013, Current stress and strain-rate fields across the Dead Sea Fault System: Constraints from seismological data and GPS observations: Earth and Planetary Science Letters, v. 369-370, p. 305–316, doi: 10.1016/j.epsl.2013.03.043.

Pavlis, G.L., 1986, Appraising earthquake hypocenter location errors: A complete, practical approach for single-event locations: Bulletin of the Seismological Society of America, v. 76, no. 6, p. 1699–1717.

Pavlis, G.L., Vernon, F., Harvey, D., and Quinlan, D., 2004, The generalized earthquake-location (GENLOC) package: An earthquake-location library: Computers and Geosciences, v. 30, no. 9-10, p. 1079–1091, doi: 10.1016/j.cageo.2004.06.010.

Plenefisch, T., and Bonjer, K.-P., 1997, The stress field in the Rhine Graben area inferred from earthquake focal mechanisms and estimation of frictional parameters: Tectonophysics, v. 275, no. 1–3, p. 71–97, doi: http://dx.doi.org/10.1016/S0040-1951(97)00016-4.

Polozov, A., and Pinsky, V., 2004, New software for seismic network and array data processing and joint seismological data base. First year report GII 546/075/04. Prepared for the Ministry of National Infrastructures:.

505 Quennell, A.M., 1956, Tectonics of the Dead Sea rift: Congreso Geologico
506 Internacional, 20th sesion, Asociacion de Servicios Geologicos Africanos, p.
507 358–405.

508 Ranalli, G., 1995, Rheology of the Earth: Springer Science & Business Media.

509 Ron, H., 1987, Deformation along the Yammuneh, The restraining bend of the Dead
510 Sea Transform: Paleomagnetic data and kinematic implications: Tectonics, v. 6,
511 no. 5, p. 653, doi: 10.1029/TC006i005p00653.

512 Rybakov, M., Goldshmidt, V., and Rotstein, Y., 1997, New regional gravity and
513 magnetic maps of the Levant: Geophysical Research …, v. 24, no. 1, p. 33–36.

514 Sadeh, M., Hamiel, Y., Ziv, A., Bock, Y., Fang, P., and Wdowinski, S., 2012, Crustal
515 deformation along the Dead Sea Transform and the Carmel Fault inferred from
516 12 years of GPS measurements: Journal of Geophysical Research, v. 117, no.
517 B8, p. 1–14, doi: 10.1029/2012JB009241.

518 Sato, T., Kasahara, J., Taymaz, T., Ito, M., Kamimura, A., Hayakawa, T., and Tan,
519 O., 2004, A study of microearthquake seismicity and focal mechanisms within
520 the Sea of Marmara (NW Turkey) using ocean bottom seismometers (OBSs):
521 Tectonophysics, v. 391, no. 1-4 SPEC.ISS., p. 303–314, doi:
522 10.1016/j.tecto.2004.07.018.

523 Segev, A., and Rybakov, M., 2011, History of faulting and magmatism in the Galilee
524 (Israel) and across the Levant continental margin inferred from potential field
525 data: Journal of Geodynamics, v. 51, no. 4, p. 264–284, doi:
526 10.1016/j.jog.2010.10.001.

527 Segev, A., Rybakov, M., Lyakhovsky, V., Hofstetter, A., Tibor, G., Goldshmidt, V.,
528 and Ben-Avraham, Z., 2006, The structure, isostasy and gravity field of the
529 Levant continental margin and the southeast Mediterranean area:
530 Tectonophysics, v. 425, no. 1-4, p. 137–157, doi: 10.1016/j.tecto.2006.07.010.

531 Shalev, E., Lyakhovsky, V., Weinstein, Y., and Ben-Avraham, Z., 2013, The thermal
532 structure of Israel and the Dead Sea Fault: Tectonophysics, v. 602, p. 69–77, doi:
533 10.1016/j.tecto.2012.09.011.

534 Shamir, G., 2006, The active structure of the Dead Sea Depression: Geological
535 Society of America, v. Special Pa, no. 02, p. 15–32, doi: 10.1130/2006.2401(02).

536 Shamir, G., Baer, G., and Hofstetter, A., 2003, Three-dimensional elastic earthquake
537 modelling based on integrated seismological and InSAR data : the M w = 7 . 2
538 Nuweiba earthquake , gulf of Elat / Aqaba 1995 November: Transform, p. 731–
539 744.

540 Shapira, A., Avni, R., and Nur, A., 1993, New estimate of the Jericho earthquake
541 epicenter of July 11, 1927: Israel Journal of Earth Sciences, v. 42, no. July 1927,
542 p. 93–96.

Shapira, A., and Hofstetter, R., 2007, Earthquake hazard assessments for building codes:.

Shearer, P.M., Hauksson, E., and Lin, G.Q., 2005, Southern california hypocenter relocation with waveform cross-correlation, part 2: Results using source-specific station terms and cluster analysis: Bulletin of the Seismological Society of America, v. 95, no. 3, p. 904–915, doi: 10.1785/01200401168.

Sibson, R.H., 1982, Fault zone models, heat flow, and the depth distribution of earthquakes in the continental crust of the United States: B. Seismol. Soc. Am., v. 72, no. 1, p. 151–163.

de Vicente, G., Cloetingh, S., Muñoz-Martín, a., Olaiz, a., Stich, D., Vegas, R., Galindo-Zaldívar, J., and Fernández-Lozano, J., 2008, Inversion of moment tensor focal mechanisms for active stresses around the microcontinent Iberia: Tectonic implications: Tectonics, v. 27, no. 1, p. n/a–n/a, doi: 10.1029/2006TC002093.

Waldhauser, F., and Ellsworth, W.L., 2000, A double-difference earthquake location algorithm: Method and application to the northern Hayward fault, California: Bulletin of the Seismological Society of America, v. 90, no. 6, p. 1353–1368.

Weber, M., Ayyash, K.A., Abueladas, A., Agnon, A., Al-Amoush, H., Babeyko, A., Bartov, Y., Baumann, M., Ben-Avraham, Z., Bock, G., Bribach, J., El-Kelani, R., Forster, A., Forster, H.J., et al., 2004, The crustal structure of the Dead Sea Transform: Geophysical Journal International, v. 156, no. 3, p. 655–681, doi: 10.1111/j.1365-246X.2004.02143.x.

Wetzler, N., Marco, S., and Heifetz, E., 2010, Quantitative analysis of seismogenic shear-induced turbulence in lake sediments: Geology, v. 38, no. 4, p. 303–306, doi: 10.1130/g30685.1.

Wetzler, N., Sagy, A., and Marco, S., 2014, The Association of Micro-earthquake Clusters with Mapped Faults in the Dead Sea Basin: Journal of Geophysical Research, v. 119, no. 11, p. 1–19, doi: 10.1002/2013JB010877.

Zaliapin, I., and Ben-Zion, Y., 2013, Earthquake clusters in southern California I: Identification and stability: Journal of Geophysical Research: Solid Earth, , no. 8004, p. n/a–n/a, doi: 10.1002/jgrb.50179.

Appendix

We examined several 1-D velocity models that were used in the past 20 years, for the location of seismic activity in the region of Israel. These models include: 1) Feigin and Shapira 1994, which we name JStar, 2) Aldersons et al. 2003, 3) Gitterman et al. 2005, named GITT05, 4) Mechie et al. 2009, which we call Desire-2009, 5) Kennett and Engdahl, 1991, named here IASP91. The first four models are considered local velocty models while the IASP91 is well-known and is considered appropriate for regional to global scale velocity models.

The Feigin and Shapira (1994) velocity model, was generated according to a set of explosions made during the ealry years of the ISN and recorded by the ISN stations. The Aldersons-2003 velocity model was comprised from three velocity models: for the Dead Sea Basin, for Israel, and for Jordan. We examined the Israel model which was derieved from quarry blasts located in the vicinity of the Dead Sea basin. The GITT05 velocity model provides the most comprehensive work, done to date, treating the entire region of the DSF, using a set of controlled explosions recorded by all network stations, including stations in Israel, Jordan, Cyprus, and Turkey. Therefore, although considered a local velocity model, it contains many regional features. The Desire-2009 model is a model that was generated mainly for the Dead Sea Basin, including some features that are to the east and west of the Dead Sea Basin, but does not consider the variations to the north and south of the Basin.

Figure A1 shows the five P-velocity models we have examined in this study. Note that the variation between the different models is mainly within the upper 5km of the crust, showing a ~ 3 – 6 km/s range, in which the higher velocity is seen for the IASP91 regional velocity model. This is an important observation in the sense that it

reflects the strong influence of the Dead Sea sedimantary basin on the generation of the velocity models, which for three of the models is rather significant: JStar, Desire-2009 and Aldersons-2003.

Figure A2 presnts the focal depth distribution for the five velocity models, compared also to the original locations of the catalogoue. The main observation, which is also discussed in the main section of the text, is that in the original catalogue, 90% of the events occur at very shallow depth (0-5km). This has no geologic or seismotectonic justification, and contraditcs previous and more focused studies done in the region (e.g., Aldersons et al., 2003; Hofstetter et al., 2012; Wetzler et al., 2014). The second observation is that Aldersons-2003 seemed to do a very reasonable job in the depth distribution, even better than IASP91 and GITT05. However, mapping the Aldersons-2003 relocations provides a very strong shift of all the southern events, to the east (Figure A3). These new relocations cannot be supported by any other evidences, and on the contrary, seem to be an artifact generated from the misfit of the Aldersons model to the high seismic velocity of the igneous lithology in Southern Israel and Jordan. Therefore, Aldersons-2003 was rejected, and based on Figure A2, GITT05 and IASP91, were the best two other candidates, with a reasonable focal depth distribution, and hence were chosen for further analysis, discussed in detail in the main text.

Tables

Table 1: Median values of locations and relocations misfits

Median values of locations and relocations misfits (measured in km) calculated for a) the initial locations, and for the Antelope relocations using b) IASP91 global velocity model, and c) GITT05 local velocity model (Gitterman et al., 2005). Errors are presented in kilometers for four distribution types: All events, In-Network events, Off-Network-N events and the Off-Network-S events. The area of the In-Network events is presented by the rectangle in Figure 3.

630 **Figures**

631

632 **Figure 1:** a) Map of the Middle East, including the regional major fault systems
633 (black lines). The regional tectonic plate configuration is presented along with the
634 relative horizontal slip motions (black arrows). The research area is marked by the
635 gray rectangle; b) The regional seismic stations that were operational within the
636 period of 1985 – 2015, including those of the Israel Seismic Network (dark gray
637 circles– short period, black triangles - broadband), and those of the Jordanian Seismic
638 Observatory (light gray diamonds).

639

640 **Figure 2:** a) The earthquake catalog recorded by the GII between 1985 and 2015,
641 having a total of 15856 events. Filled circles show the original locations of the
642 seismic events, with their size scaled by magnitude. The 1995 M7.2 earthquake is
643 presented with the focal mechanism (strike: 222, dip: 77, rake: -15) according to
644 Hofstetter et al. 2003. The inset '*b*' shows the seismic P-wave velocity models applied
645 for the region. The initial location was obtained by JStar's software model (line with
646 diamonds) and for the relocations we used the velocity model of Gitterman et al.
647 (2005) (GITT05 - black line); the IASP91 global crustal model is given here for
648 reference (dashed line).

649

650 **Figure 3**: The relocated catalog, based on the P and S arrivals recorded by the
651 GII between 1985 and 2015, with a total of 15181 events. Filled circles show the
652 relocated seismic events, with their size scaled by magnitude. The coverage area of

653 the seismic network is marked by the black dashed rectangle; beyond this area,
654 locations are poorly constrained**.** b) Depth histograms of the original (white-
655 'Catalog'), relocated events using Gitterman et al. (2005) velocity model (GITT05 -
656 black), and relocated events using IASP91 velocity model (gray), of four catalog
657 types: b1) all events, b2) events within the coverage area (In-Network), b3) Off-
658 Network North events, and b4) Off-Network South events.

659

660 **Figure 4**: Location errors for the two velocity models: IASP91 in dashed histograms,
661 and GITT05 (following Gitterman et al., 2005) in black, for three geographical axes:
662 a) X-axis (East-West), b) Y-axis (North-South), and c) Vertical axis, and for three
663 data sets: 1-All, 2-In Network, and 3-off Network. The mean median calculated for
664 the two velocity models is shown by the black vertical line in all nine subplots and
665 presented by the absolute value of the difference between the two models.

666

667 **Figure 5:** The horizontal location shifts for two velocity models are presented, using
668 the JStar original locations as the reference for these shifts. The upper row (a1 and a2)
669 are for the relocations obtained by the velocity model of Gitterman et al. (2005), and
670 the middle row (b_1 and b_2) are for the relocations obtained by IASP91. The rose
671 diagrams, a_1 and b_1, show the azimuthal shifts measured from the earthquake initial
672 location to the new location; the radius of the 20° slices mark the number of events
673 within the slice, and the contours are of the number of events (500, 1000)**.** The polar
674 diagrams, a_2 and b_2, show the median shifts for each direction (in km) for several
675 subsets of the data: all events (blue), in-grid events - located within the coverage area
676 (magenta); off-grid events - located north of the coverage area (light blue), and off-

grid events - located south of the coverage area (green). Dashed circles present the total medians shift: a2) 4.6, 1.8, 4.4 and 8.2 km for Gitterman 2005 velocity model, and b2) 5.9, 2.2, 5.5, and 8.9 km for IASP91, respectfully; c) Cross section emphasizing the S-N horizontal shifts of the off-grid events - located south of the coverage area.

Figure 6: The seismogenic zone along the DSF; the dashed gray line in (b), is plotted by gray lines in (a) according to a moving quantile of 0.75 (solid), and 0.95 (dashed), applying a window of 10 km (~N-S axis) by 15 km (~E-W), in 5 km intervals. The two black lines are the temperature contours of 300 °C and 350 °C calculated by Shalev et al. (2013) along the DSF, and marked by the black dashed line in (b).

Figure A1: The five velocity model examined in this study and presented by the P-wave velocity: 'IASP91' is based on Kennett and Engdahl (1991); 'Aldersons-2003' is based on the Israel model suggested by Aldersons et. al. (2003); 'JStar' is by Feigin and Shapira (1994); 'GITT05' is as suggested by Gitterman et. al. (2005); 'Desire-2009' is composed by Mechie et. al (2009).

Figure A2: The focal depth distribution for the five velocity models described in Figure A1, including the original locations of the catalog ('Original').

Figure A3: The relocated catalog, based on the P and S arrivals recorded by the GII between 1985 and 2015, with a total of 14849 events, located based on the Israel velocity model suggested by Aldersons et al. (2003). Filled circles show the new locations of the seismic events, with their size scaled by magnitude.

Median values of locations and relocations misfits

	Location (JStar)				Relocation (IASP91)				Relocation (GITT05)			
	Events	Err x	Err y	Err z	Events	Err x	Err y	Err z	Events	Err x	Err y	Err z
All	15856	8.4	4.0	6.0	15150	0.77	1.05	1.30	15181	0.72	1.00	1.26
In-Network	6576	2.3	1.3	2.2	5909	0.44	0.56	0.78	6223	0.43	0.55	0.76
Off-Network-N	1447	6.5	3.2	3.2	1783	0.71	0.86	1.14	1528	0.78	1.06	1.31
Off-Network-S	7833	135.0	17.0	30.0	7454	1.47	1.83	2.35	7430	1.39	1.74	2.27

Table 1: Median values of locations and relocations misfits (measured in km) calculated for a) the initial locations, and for the Antelope relocations using b) IASP91 global velocity model, and c) GITT05 local velocity model (Gitterman et al., 2005). Errors are presented in kilometers for four data subsets: ***All*** events, ***In-Network*** events, ***Off-Network-N*** events and the ***Off-Network-S*** events. The area of the ***In-Network*** events is presented by the rectangle in Figure 3.

Figure-1
Click here to download Figure: Fig_1_MedEast_STN_bnw.png

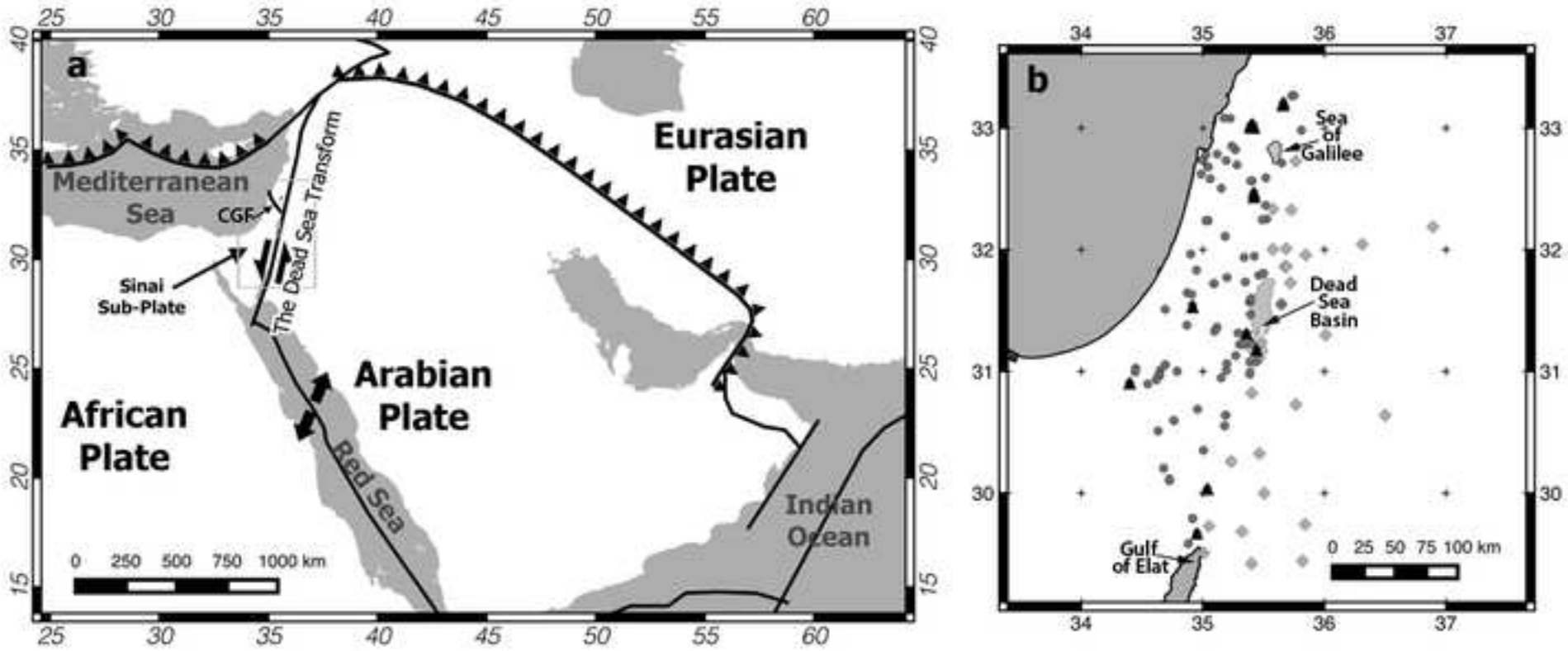

Figure-2
Click here to download Figure: Fig_2_JStar_GII.tif

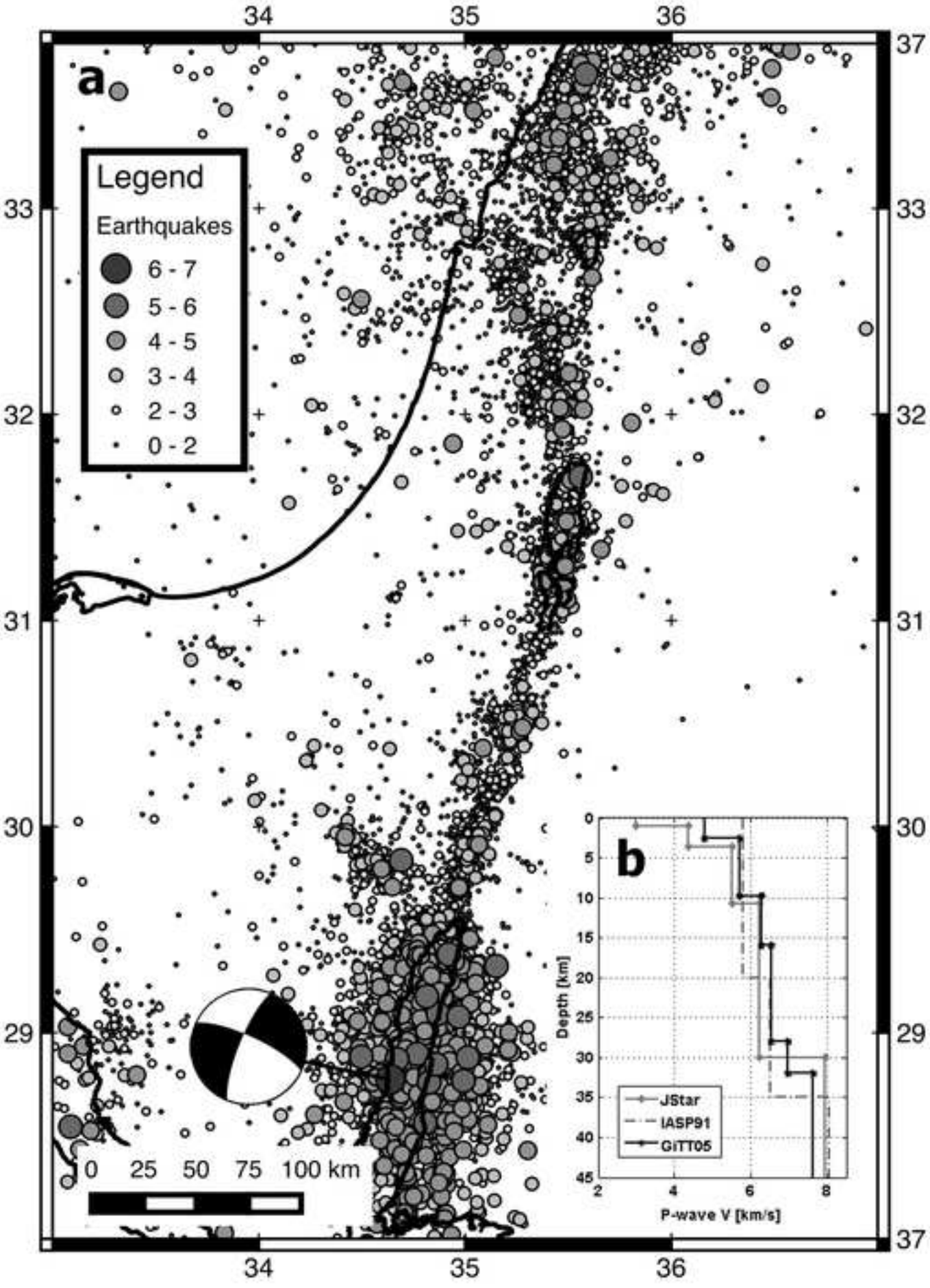

Figure-3

Click here to download Figure: Fig_3_Git05_loc_Depth_Hist_bnW1.tif

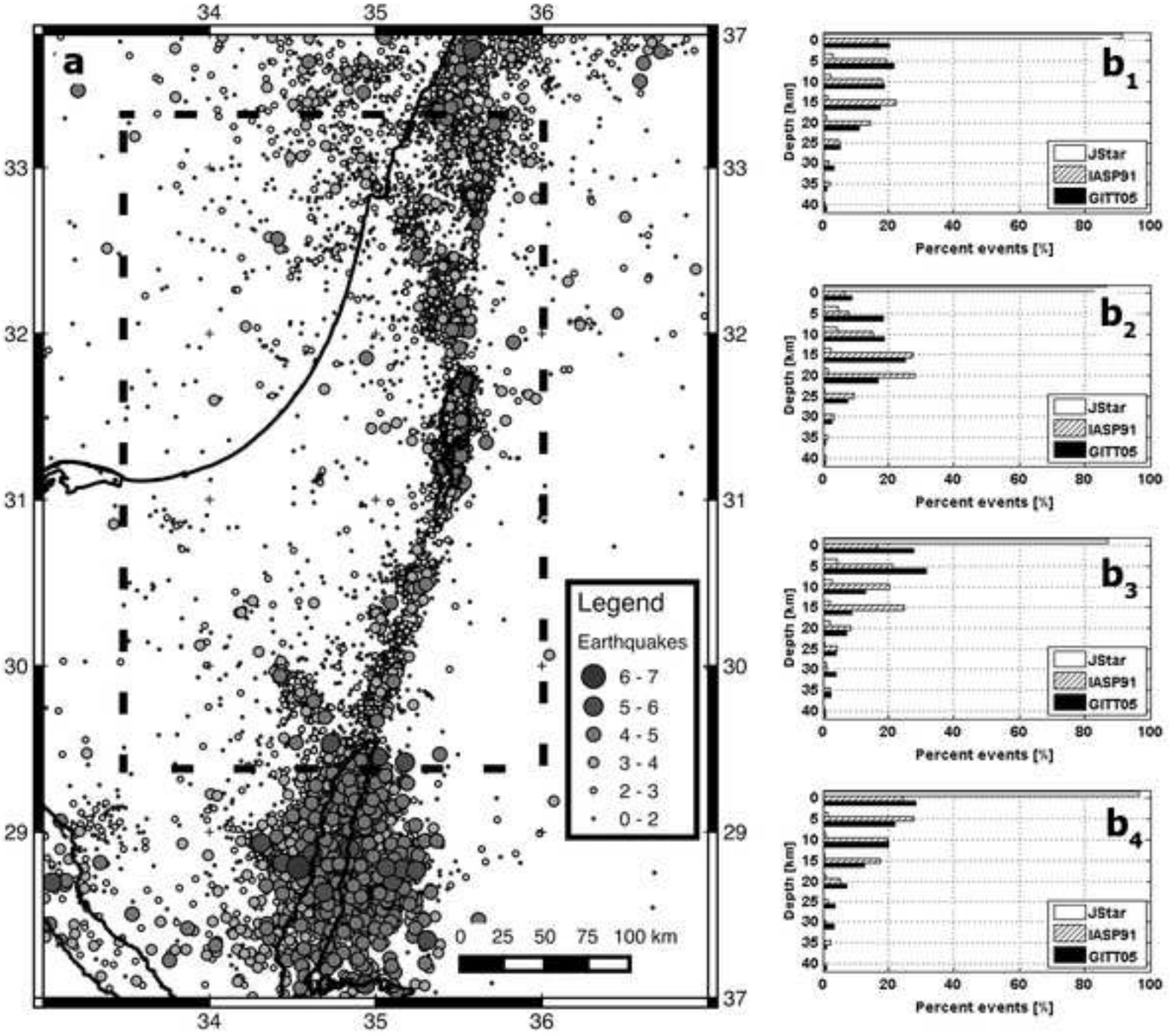

Figure-4

Click here to download Figure: Fig_4_Errors_3x3.tif

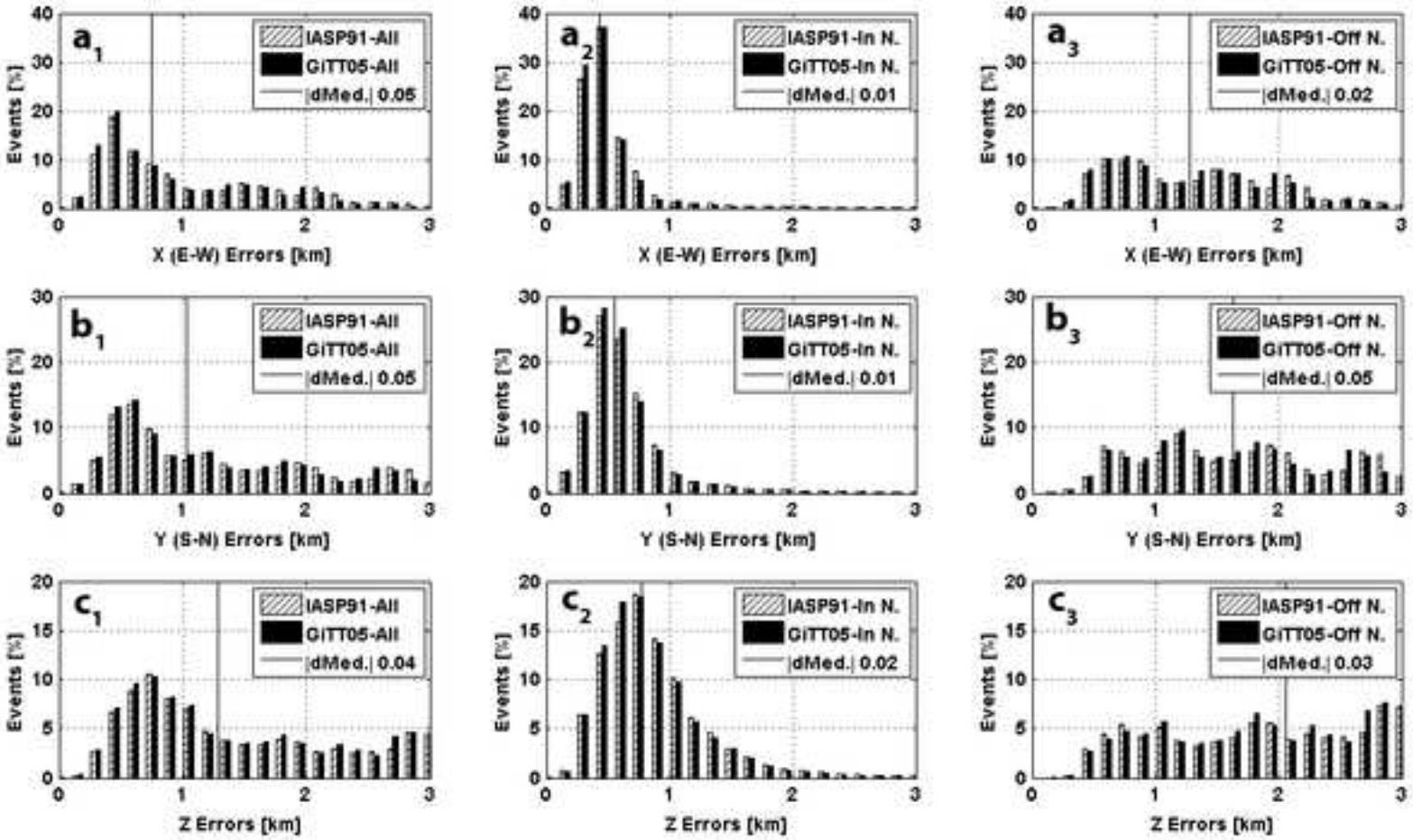

Figure-5
Click here to download Figure: Fig_5_Shifts4.tif

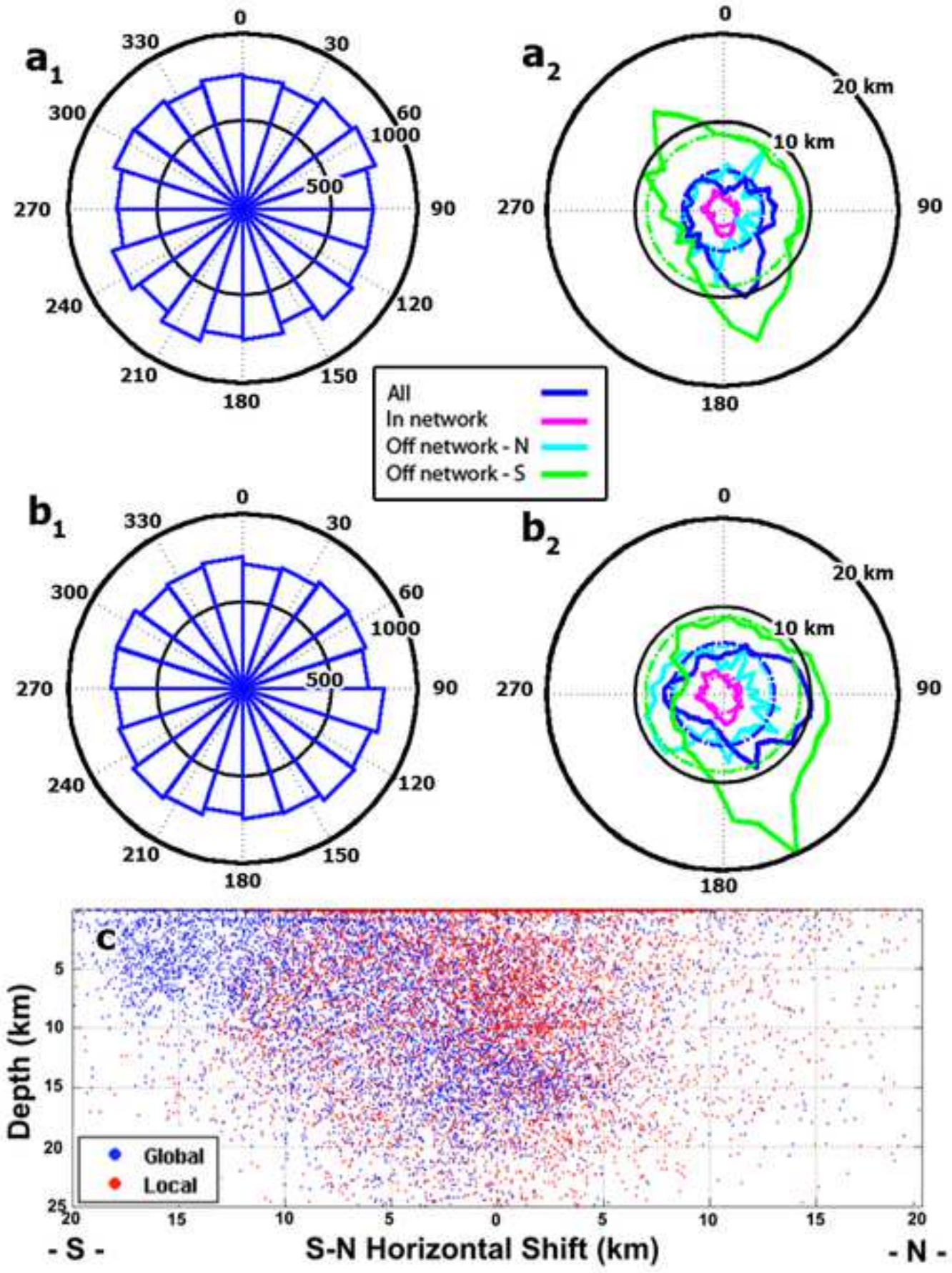

Figure-6
Click here to download Figure: Fig_6_SeismogenicZ_Q0.75_0.95_bnw.tif

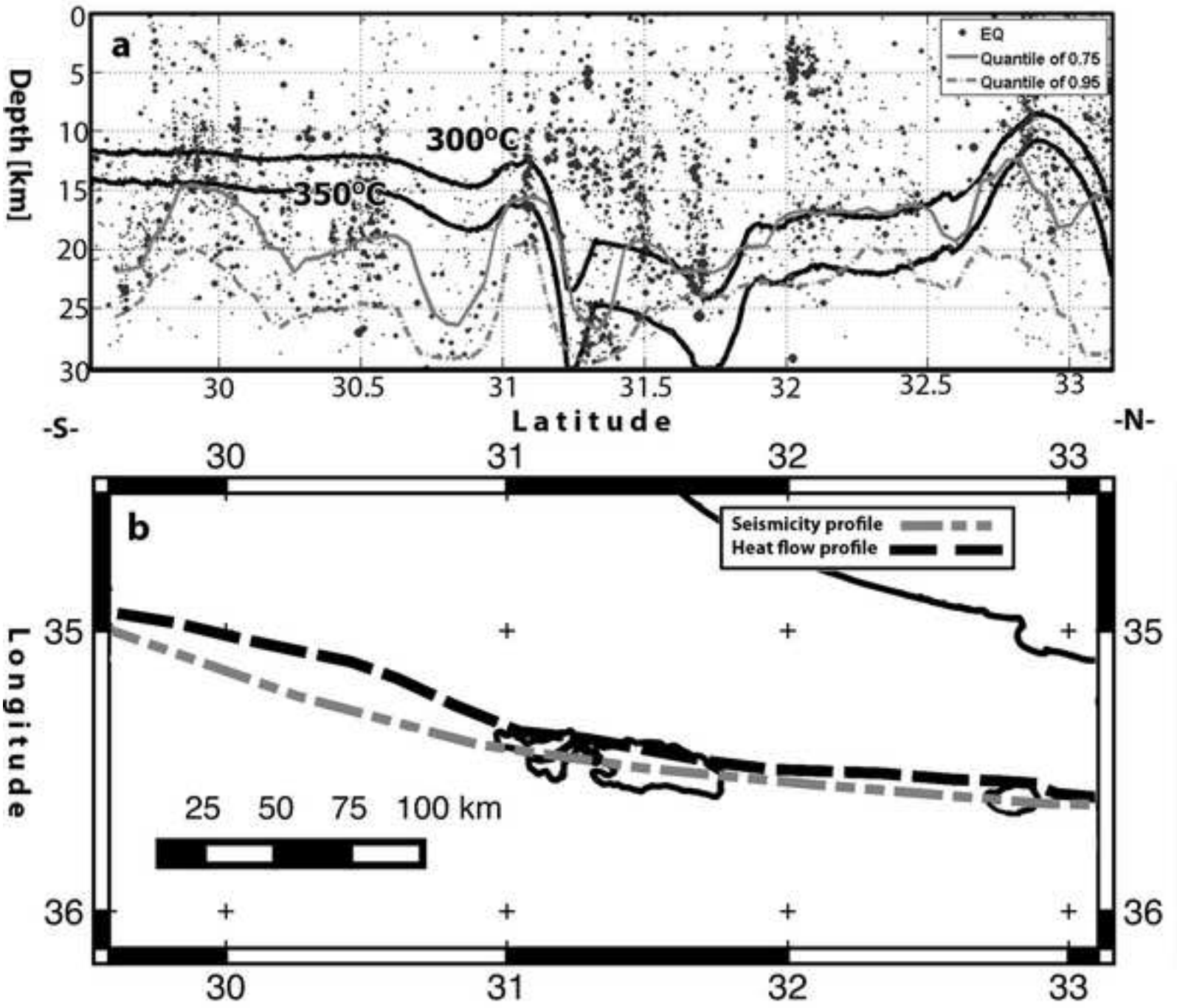

Figure-A1
Click here to download Figure: A1-Vmodels.png

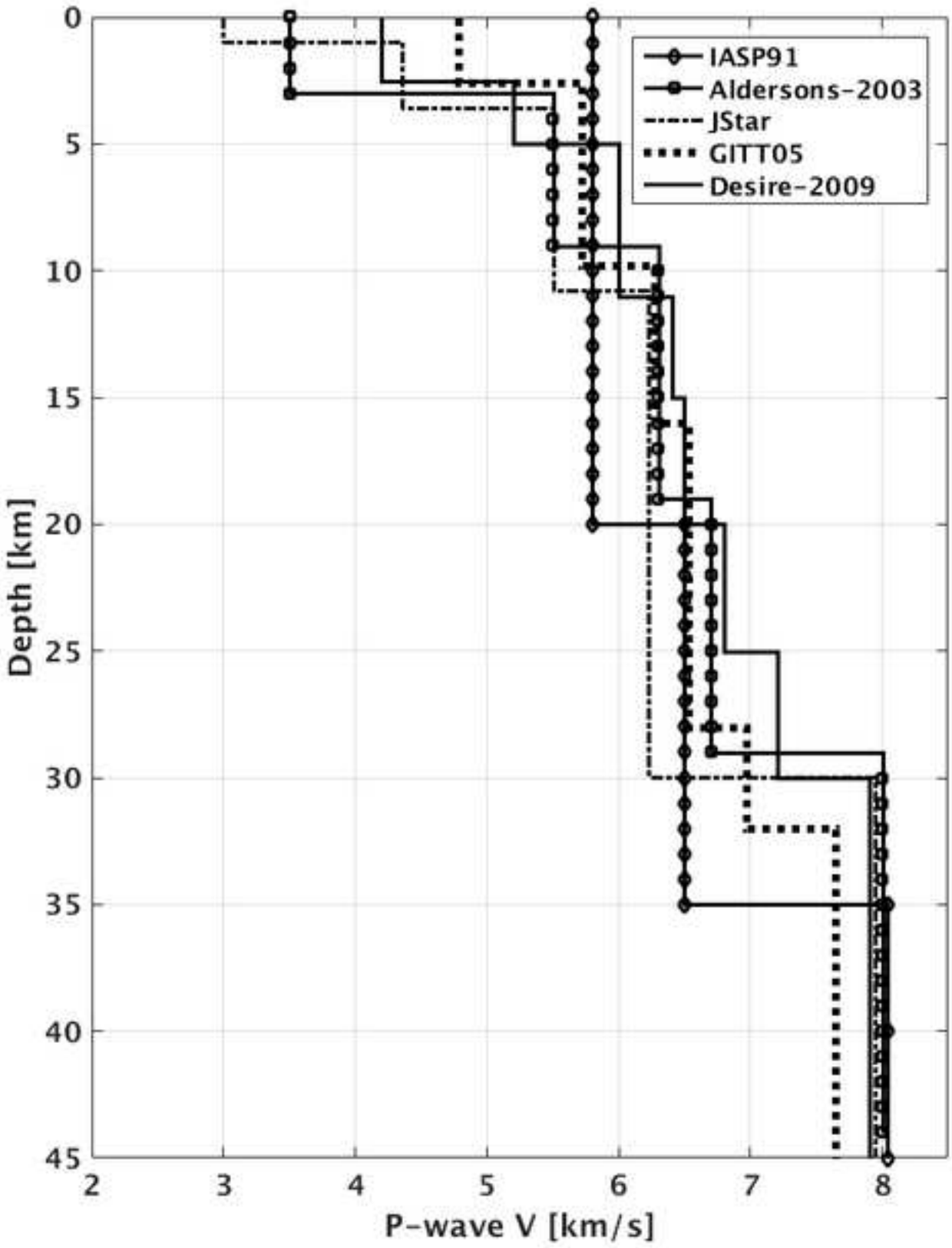

Figure-A2
Click here to download Figure: A2-Depth_All_BnW.png

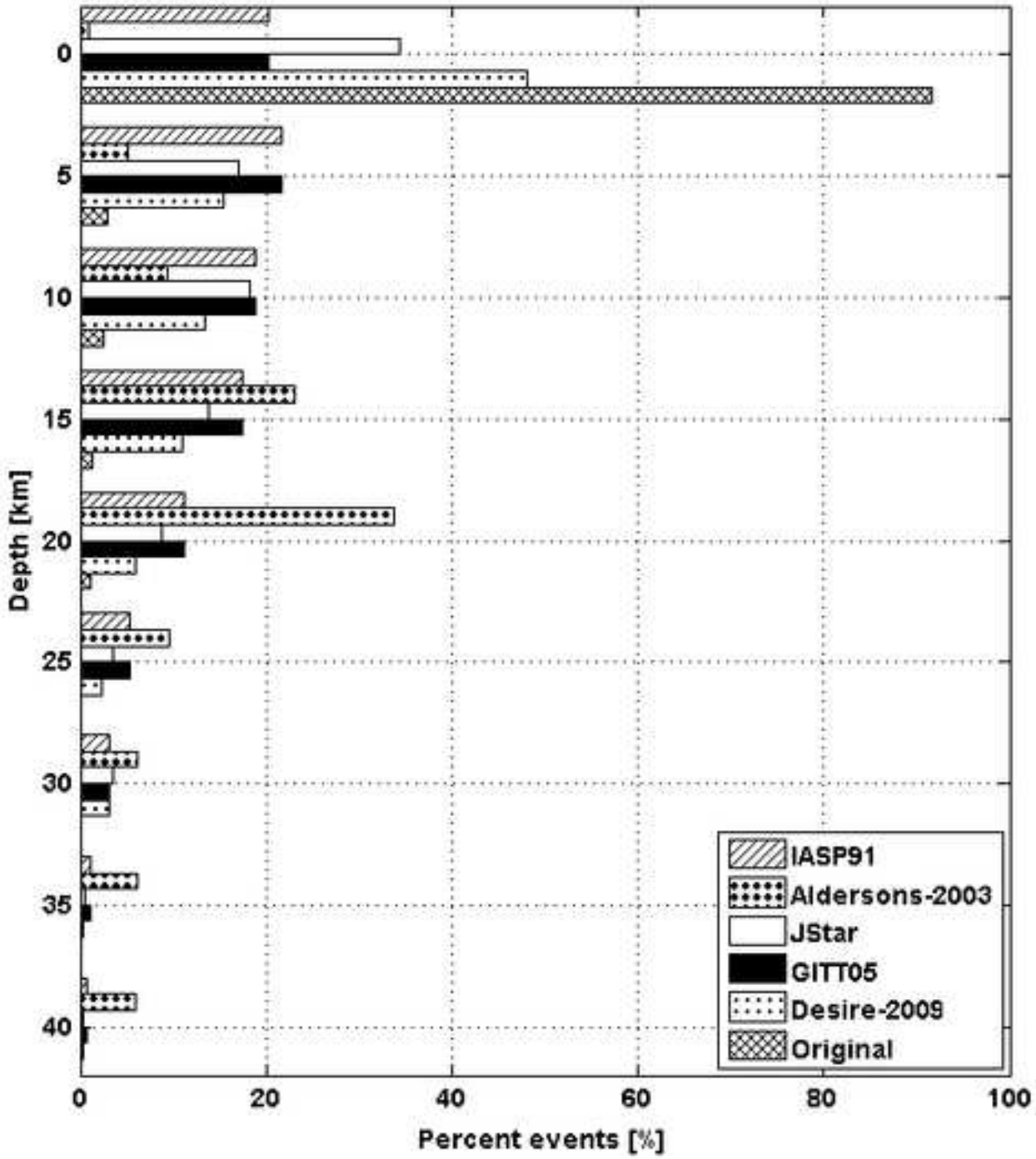

Figure-A3
Click here to download Figure: A3-Aldersons_BnW.jpg

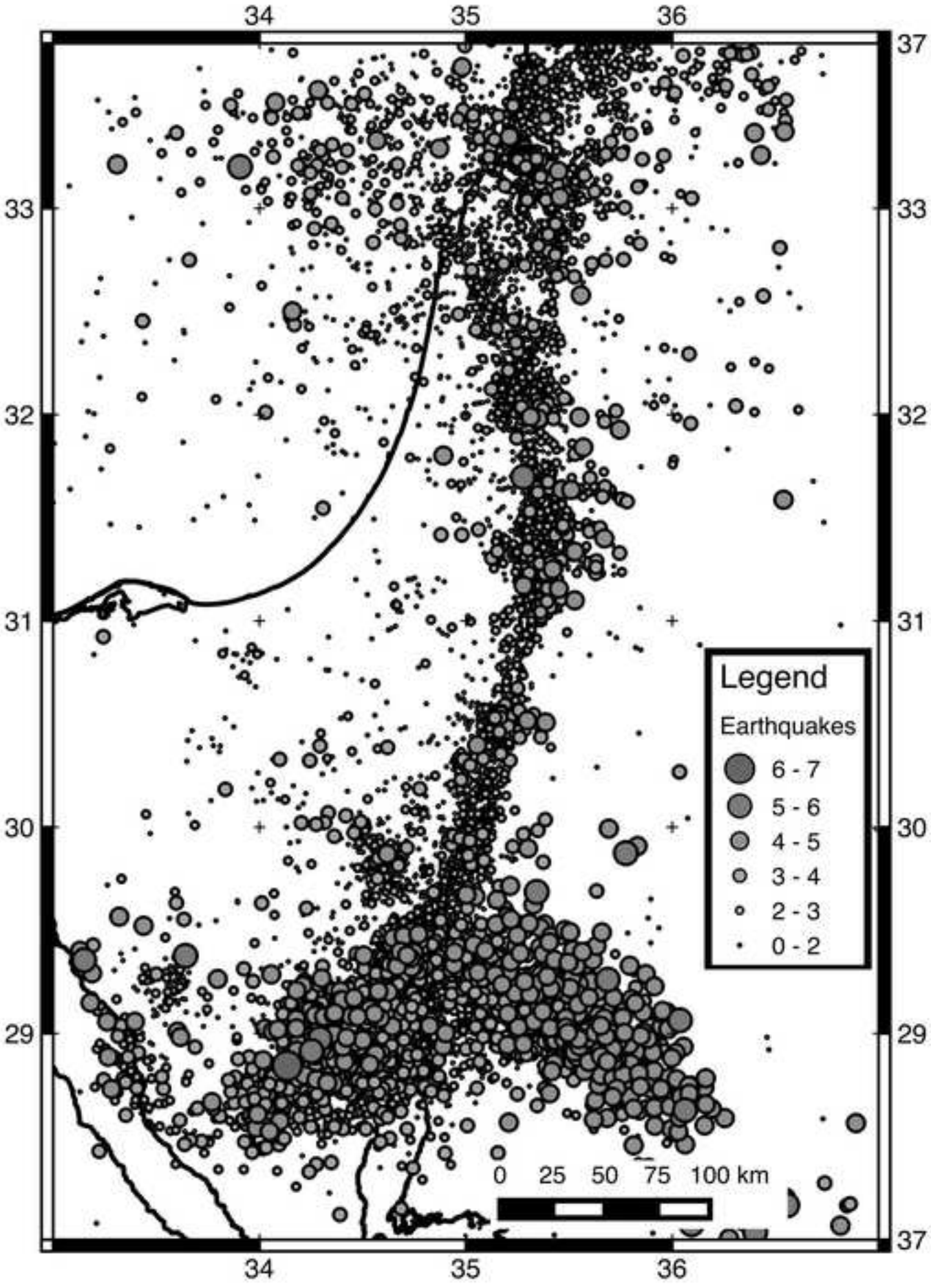

תקציר

יותר מ-15,000 אירועים סיסמיים, בקרבת העתק ים-המלח, תועדו ע"י הרשת הסיסמית הישראלית (ISN) ב- 30 שנות פעילותה. במהלך שנים אילו, איכון האירועים נעשה תוך שימוש במודלים שונים של מהירות תת-הקרקע, וכתוצאה מכך, איכון האירועים אינו עקבי. בנוסף, גילינו שלפחות בקטלוג הסיסמי המתפרסם ע"י האגף לסיסמולוגיה, העומקים של האירועים הסיסמיים נוטים להיות רדודים מדי ביחס למצופה מהסביבה הטקטונית, וביחס למחקרים ממוקדים יותר שנעשו בעבר לאורך העתק ים-המלח. מכאן שיש ערך רב בשיפור האיכון של האירועים הסיסמיים, וזהו תנאי הכרחי ומחייב הדרוש לקביעת התכונות והמאפיינים של המקורות הטקטוניים בישראל, והערכת הסיכונים הסיסמיים באזורנו. בשלב זה במחקרנו התמקדנו בשיפור איכון רעידות האדמה באזורינו, בעזרת: א. תוכנת איכון סיסמית (כחלק מתוכנת העיבוד: Antelope) המאכנת כל אירוע בנפרד (single event location), ו- ב. שימוש בשני מודלים שונים למהירות הסיסמית בתת-הקרקע, האחת מקומית (Gitterman et al. 2005), והשנייה גלובאלית. ואכן, האיכון המחודש שעשינו, הראה תפוצת אירועים עקבית וסבירה יותר לאזורינו, עם עומקים המתאימים לממצאים שעלו במחקרים קודמים. כמו-כן, אנו מנצלים במה זו על מנת לחקור כיצד האיכון מושפע מהפריסה של התחנות הסיסמיות ביחס למיקום האירועים, כאשר האפקט העיקרי הוא שאירועים המתרחשים תחת כיסוי טוב של תחנות הרשת הסיסמית "זוכים" לאיכון מוצלח גם מבחינת העומקים, בעוד שבמקרים של כיסוי פחות מוצלח (כגון תחנות דרום הארץ המתעדות רעידות במפרץ סואץ), הייתה הטיה לאיכונים רדודים מהצפוי, ולוודאות מיקום נמוכה יותר. העומקים המתקבלים באיכון המחודש המוצג בעבודה זו מראים התאמה טובה יותר לאזורים הסיסמוגניים, כפי שהוצגו במחקרים קודמים, אם בתחום הסיסמולוגיה אם במחקרים המבוססים על שפיעת חום בהעתק ים המלח.

הקטלוג המחודש נחשב לאיכון הטוב והמקיף ביותר שנעשה לאירועים הסיסמיים בישראל, ומהווה תשתית הכרחית לכל מחקר עתידי בתחום, וכתנאי התחלה לשיטות איכון מורכבות יותר. האיכון המחודש ייפתח בקרוב לקהל הרחב להורדה כשכבות של מערכות מידע גיאוגרפיות כגון GIS ו- Google Earth, באתר המכון הגיאולוגי: https://www.gsi.gov.il. שלב ראשוני זה של המחקר סוכם לכדי מאמר שהתקבל לאחרונה לפרסום בכתב עת בינלאומי ומקצועי בתחום הסיסמולוגיה (Seismological Research Letters – SRL), ומצורף כנספח לדו"ח זה.

הערכת סיכונים סיסמיים של מקורות טקטוניים בישראל: מהערכת סיכונים כללית ועד להערכה ממוקדת לתחנות כוח גרעיניות

דו"ח מדעי, שנה ראשונה – נובמבר 2015

שיפור איכון רעידות האדמה ב- 30 השנים האחרונות והערכה טובה יותר של האזורים הסיסמוגניים לאורך ובקרבת העתק ים המלח

איתי קורזון ונדב וצלר

המכון הגאולוגי

משרד התשתיות הלאומיות, האנרגיה והמים

תקציבים: 003-17-212 ו- 010-11-214.